Bibliography

Abdel-azim, A. G., & Abdel-azim, G. A. (2016). The Impact of Antibiotic Exposure and Concentration on Resistance in Bacteria. *Journal of Emerging Investigators*, *7*, 2–7.

Agarwal, N., Verma, I., Siddiqui, N., & Javed, S. (2021). Experimental spectroscopic and quantum computational analysis of pyridine-2,6-dicarboxalic acid with molecular docking studies. *Journal of Molecular Structure*, *1245*, 131046. https://doi.org/10.1016/j.molstruc.2021.131046

Ahmet, Ç., Ali, E.S., Mehmet, M. A., Yunus Z., Muhammet, U.K. (2021) Porphyrin-based covalent organic polymer by inverse electron demand Diels-Alder reaction. *European Polymer Journal*, 157 (15),110664

Alanine, T. A., Galloway, W. R. J. D., Bartlett, S., Ciardiello, J. J., McGuire, T. M., & Spring, D. R. (2016). Concise synthesis of rare pyrido[1,2-a]pyrimidin-2-ones and related nitrogen-rich bicyclic scaffolds with a ring-junction nitrogen. *Organic and Biomolecular Chemistry*, *14*(3), 1031–1038. https://doi.org/10.1039/c5ob01784j

Albrecht, Ł., Dickmeiss, G., Weise, C. F., Rodríguez-Escrich, C., & Jørgensen, K. A. (2012). Dienamine-mediated inverse-electron-demand hetero-diels-alder reaction by using an enantioselective H-bond-directing strategy. *Angewandte Chemie - International Edition*, *51*(52), 13109–13113. https://doi.org/10.1002/anie.201207122

Anderson, E. D., & Boger, D. L. (2011). Inverse electron demand diels-alder reactions of 1,2,3-triazines: Pronounced substituent effects on reactivity and cycloaddition scope. *Journal of the American Chemical Society*, *133*(31), 12285–12292. https://doi.org/10.1021/ja204856a

Arvinnezhad, H., Ghorbani, F., Khosravi, H., Jadidi, K., Notash, B., & Naderi, S. (2020). Exo/endo stereocontrolled synthesis of spiroindoloindolizidines by using classical and microwave conditions via the 1,3-dipolar cycloaddition reaction. *Journal of Heterocyclic Chemistry*, *57*(8), 3222–3229. https://doi.org/10.1002/jhet.4005

Avcı, Ö. N., Catak, S., Dereli, B., Aviyente, V., & Dedeoglu, B. (2020). Elucidation of the Mechanism of Silver-Catalyzed Inverse Electron-Demand Diels-Alder (IEDDA) Reaction of 1,2-Diazines and Siloxy Alkynes. *ChemCatChem*, *12*(1), 366–372. https://doi.org/10.1002/cctc.201901525

Awouters, F., Vermeire, J., Smeyers, F., Vermote, P., van Beek, R., & Niemegeers, C. J. E. (1986). Oral antiallergic activity in ascaris hypersensitive dogs: A study of known antihistamines and of the new compounds ramastine (R 57 959) and levocabastine (R 50 547). *Drug Development Research*, *8*(1–4), 95–102. https://doi.org/10.1002/ddr.430080112

Babu, G., & Perumal, P. T. (1998). Convenient synthesis of pyrano[3,2-c]quinolines and indeno[2,1- c]quinolines by imino Diels-Alder reactions. *Tetrahedron Letters*, *39*(20), 3225–3228. https://doi.org/10.1016/S0040-4039(98)00397-9

Balaban, A. T., Oniciu, D. C., & Katritzky, A. R. (2004). Aromaticity as a cornerstone of heterocyclic chemistry. *Chemical Reviews*, *104*(5), 2777–2812. https://doi.org/10.1021/cr0306790

Beeck, S., & Wegner, H. A. (2022). Mechanistic Studies on the Bidentate Lewis Acid Catalyzed Domino Inverse Electron-Demand Diels-Alder/Thiol Transfer Reaction. *European Journal of Organic Chemistry*. https://doi.org/10.1002/ejoc.202201289

Biagiotti, G., Legnani, L., Aresta, G., Chiacchio, M. A., & Richichi, B. (2022). Benzo[c][1,2]thiazine-Based Analogs in the Inverse Electron Demand [4+2] Hetero Diels-Alder Reaction with Glycals: Access to Tetracyclic Fused Galactose and Fucose Derivatives. *European Journal of Organic Chemistry*, *2022*(43). https://doi.org/10.1002/ejoc.202200769

Bielecki, J., & Lipiec, E. (2016). Basis set dependence using DFT/B3LYP calculations to model the Raman spectrum of thymine. *Journal of Bioinformatics and Computational Biology*, *14*(1), 1–15. https://doi.org/10.1142/S0219720016500025

Branowska, D. (2003). A facile route to symmetrical and unsymmetrical cycloalkeno[c]fused 2,2′-bipyridine ligands via inverse electron demand diels-alder reaction of 5,5′-bi-1,2,4-triazines. *Synthesis*, *13*, 2096–2100. https://doi.org/10.1055/s-2003-41452

Buttard, F., Berthonneau, C., Hiebel, M. A., Brière, J. F., & Suzenet, F. (2019). Organocatalytic aza-Michael Reaction to 3-Vinyl-1,2,4-triazines as a Valuable Bifunctional Platform. *Journal of Organic Chemistry*, *84*(6), 3702–3714. https://doi.org/10.1021/acs.joc.9b00141

Campos, J. F., Besson, T., & Berteina-Raboin, S. (2022). Review on the Synthesis and Therapeutic Potential of Pyrido[2,3-d], [3,2-d], [3,4-d] and [4,3-d]pyrimidine Derivatives. *Pharmaceuticals*, *15*(3), 1–27. https://doi.org/10.3390/ph15030352

Canovas, C., Moreau, M., Vrigneaud, J., Collin, B., Denat, F., Goncalves, V., Canovas, C., Moreau, M., Vrigneaud, J., Bellaye, P., & Collin, B. (2021). *Modular Assembly of Multimodal Imaging Agents through an Inverse Electron Demand Diels – Alder Reaction To cite this version : HAL Id : hal-03470979*.

Chen, T., Che, C., Guo, Z., Dong, X. Q., Wang, C. J., Beeck, S., Ahles, S., Wegner, H. A., Pałasz, A., Li, J. L., Kang, T. R., Zhou, S. L., Li, R., Wu, L., Chen, Y. C., Lai, S., Mao, W., Song, H., Xia, L., … Parmar, V. S. (2015). Chiral tertiary amine thiourea-catalyzed asymmetric inverse-electron-demand Diels-Alder reaction of chromone heterodienes using 3-vinylindoles as dienophiles. *Journal of Organic Chemistry*, *51*(5), 10233–10239. https://doi.org/10.1002/chem.202104085

Cserép, G. B., Németh, K., Szatmári, Á., Horváth, F., Imre, T., Németh, K., & Kele, P. (2022). Beyond the Bioorthogonal Inverse-Electron-Demand Diels-Alder Reactions of Tetrazines: 2-Pyrone-Functionalized Fluorogenic Probes. *Synthesis (Germany)*, *54*(17), 3858–3866. https://doi.org/10.1055/a-1761-4672

Dang, A. T., Miller, D. O., Dawe, L. N., & Bodwell, G. J. (2008). Electron-deficient dienes. 5. An inverse-electron-demand Diels-Alder approach to 2-substituted 4-methoxyxanthones and 3,4-dimethoxyxanthones. *Organic Letters*, *10*(2), 233–236. https://doi.org/10.1021/ol702614b

de Geus, M. A. R., Maurits, E., Sarris, A. J. C., Hansen, T., Kloet, M. S., Kamphorst, K., ten Hoeve, W., Robillard, M. S., Pannwitz, A., Bonnet, S. A., Codée, J. D. C., Filippov, D. V., Overkleeft, H. S., & van Kasteren, S. I. (2020). Fluorogenic Bifunctional trans-Cyclooctenes as Efficient Tools for Investigating Click-to-Release Kinetics. *Chemistry - A European Journal*, *26*(44), 9900–9904. https://doi.org/10.1002/chem.201905446

Devaraj, N. K., Weissleder, R., & Hilderbrand, S. A. (2008). Tetrazine-based cycloadditions: Application to pretargeted live cell imaging. *Bioconjugate Chemistry*, *19*(12), 2297–2299. https://doi.org/10.1021/bc8004446

Di Valentin, C., Freccero, M., Sarzi-Amadè, M., & Zanaletti, R. (2000). Reactivity and endo-exo selectivity in Diels-Alder reaction of o- quinodimethanes. An experimental and DFT computational study. *Tetrahedron*, *56*(16), 2547–2559. https://doi.org/10.1016/S0040-4020(00)00126-5

Diels, O., & Kech, H. (1935). Synthesen in der hydroaromatischen Reihe. XXIV „Dien-Synthesen" stickstoffhaltiger Heteroringe. *Justus Liebigs Annalen Der Chemie*, *519*(1), 140–146. https://doi.org/10.1002/jlac.19355190112

Domingo, L. R., Aurell, M. J., & Pérez, P. (2014). The mechanism of ionic Diels-Alder reactions. A DFT study of the oxa-Povarov reaction. *RSC Advances*, *4*(32), 16567–16577. https://doi.org/10.1039/c3ra47805j

Donghi, M., Kinzel, O. D., & Summa, V. (2009). 3-Hydroxy-4-oxo-4H-pyrido[1,2-a]pyrimidine-2-carboxylates-A new class of HIV-1 integrase inhibitors. *Bioorganic and Medicinal Chemistry Letters*, *19*(7), 1930–1934. https://doi.org/10.1016/j .bmcl.2009.02.055

Dumpati, R., Vuruputuri, U., Ramatenki, V., Vadija, R., & Vellanki, S. (2018). *Structural insights into suppressor of cytokine signaling 1 protein - identification of new leads for type 2 diabetes mellitus*. *February*, 1–17. https://doi.org/10.1002/jmr.2706

Engelsma, S. B., van den Ende, T. C., Overkleeft, H. S., van der Marel, G. A., & Filippov, D. V. (2018). Reaction Rates of Various N-Acylenamines in the Inverse-Electron-Demand Diels–Alder Reaction. *European Journal of Organic Chemistry*, *2018*(20), 2587–2591. https://doi.org/10.1002/ejoc.201800094

Engelsma, S. B., Willems, L. I., Van Paaschen, C. E., Van Kasteren, S. I., Van Der Marel, G. A., Overkleeft, H. S., & Filippov, D. V. (2014). Acylazetine as a dienophile in bioorthogonal inverse electron-demand Diels-Alder ligation. *Organic Letters*, *16*(10), 2744–2747. https://doi.org/10.1021/ol501049c

Eschenbrenner-Lux, V., Kumar, K., & Waldmann, H. (2014). The Asymmetric Hetero-Diels-Alder Reaction in the Syntheses of Biologically Relevant Compounds. *Angewandte Chemie - International Edition*, *53*(42), 11146–11157. https://doi.org/10.1002/anie.201404094

Fernanda García, M., de Souza Junqueira, M., da Silva Mororó, J., Camacho, X., de Paula Faria, D., de Godoi Carneiro, C., Gallazzi, F., Chammas, R., Quinn, T., Cabral, P., & Cerecetto, H. (2021). Radio- and Fluorescent-Labeling of Rituximab Based on the Inverse Electron Demand Diels-Alder Reaction. *ChemistrySelect*, *6*(8), 1894–1899. https://doi.org/10.1002/slct.202100042

Fershtat, L. L., Larin, A. A., Epishina, M. A., Ovchinnikov, I. V., Kulikov, A. S., Ananyev, I. V., & Makhova, N. N. (2016). Design of hybrid heterocyclic systems with a furoxanylpyridine core via tandem hetero-Diels-Alder/retro-Diels-Alder reactions of (1,2,4-triazin-3-yl)furoxans. *RSC Advances*, *6*(37), 31526–31539. https://doi.org/10.1039/c6ra05110c

Fu, Z. Da, Guo, Q. H., Zhao, L., Wang, D. X., & Wang, M. X. (2016). Synthesis and Structure of Corona[6](het)arenes Containing Mixed Bridge Units. *Organic Letters*, *18*(11), 2668–2671. https://doi.org/10.1021/acs.orglett.6b01112

Fuller-Stanley, J. Liu, M. Wang, J. & Molleur, H(2003). 2-Methyl-2-di-t-butylsilyl and 2-Methyl-2-isopropylsilyl-1,3-Dithiane: 13C, 1H, 29Si NMR and Computational Studies. *RSC* 16 th International Meeting; NMR Spectroscopy, University of Cambridge, UK.June July 3, P5.7.

Fumi, S., Shota, F., and Tomoki, N. (2022). Bioorthogonal micellar nanoreactors for prodrug cancer therapy using an inverse-electron-demand Diels–Alder reaction. *Chemical Communnication.* 58, 7026-7029

García-Aznar, P., & Jorge, E. (2022) Computational insights into the inverse electron-demand Diels–Alder reaction of norbornenes with 1,2,4,5-tetrazines: norbornene substituents' effects on the reaction rate, *Organic Biomolecules of Chemistry*, 20, 6400-6412

Gaddam, V., & Nagarajan, R. (2009). A one-pot synthetic approach to the functionalized isomeric ellipticine derivatives through an imino Diels-Alder reaction. *Tetrahedron Letters*, *50*(11), 1243–1248. https://doi.org/10.1016/j.tetlet.2009.01.020

Gardiner, S. H., Lipciuc, M. L., & Vallance, C. (2015). Gas-Phase Retro-Diels-Alder Reactions of Cyclohexene, 1-Methylcyclohexene, and 4-Methylcyclohexene following Photoexcitation at 193 nm: A Velocity-Map Imaging Study. *Journal of Physical Chemistry A*, *119*(50), 12218–12223. https://doi.org/10.1021/acs.jpca.5b06185

Gaulon, C., Dhal, R., Chapin, T., Maisonneuve, V., & Dujardin, G. (2004). N-vinyl-2-oxazolidinones: Efficient chiral dienophiles for the [4 + 2]-based de novo synthesis of new N-2-deoxyglycosides. *Journal of Organic Chemistry*, *69*(12), 4192–4202. https://doi.org/10.1021/jo040102y

Ge, Y., Le, A., Marquino, G. J., Nguyen, P. Q., Trujillo, K., Schimelfenig, M., & Noble, A. (2019). Tools for Prescreening the Most Active Sites on Ir and Rh Clusters toward C-H Bond Cleavage of Ethane: NBO Charges and Wiberg Bond Indexes. *ACS Omega*. https://doi.org/10.1021/acsomega.9b02813

Gheewala, C. D., Hirschi, J. S., Lee, W. H., Paley, D. W., Vetticatt, M. J., & Lambert, T. H. (2018). Asymmetric Induction via a Helically Chiral Anion: Enantioselective Pentacarboxycyclopentadiene Brønsted Acid-Catalyzed Inverse-Electron-Demand Diels-Alder Cycloaddition of Oxocarbenium Ions. *Journal of the American Chemical Society*, *140*(10), 3523–3527. https://doi.org/10.1021/jacs.8b00260

Gil de Montes, E., Istrate, A., Navo, C. D., Jiménez-Moreno, E., Hoyt, E. A., Corzana, F., Robina, I., Jiménez-Osés, G., Moreno-Vargas, A. J., & Bernardes, G. J. L. (2020). Stable Pyrrole-Linked Bioconjugates through Tetrazine-Triggered Azanorbornadiene Fragmentation. *Angewandte Chemie - International Edition*, *59*(15), 6196–6200. https://doi.org/10.1002/anie.201914529

Goryaeva, M. V., Kushch, S. O., Khudina, O. G., Burgart, Y. V., Kudyakova, Y. S., Ezhikova, M. A., Kodess, M. I., Slepukhin, P. A., Sadretdinova, L. S., Evstigneeva, N. P., Gerasimova, N. A., & Saloutin, V. I. (2019). Autocatalyzed three-component cyclization of polyfluoroalkyl-3-oxo esters, methyl ketones and alkyl amines: A novel approach to 3-alkylamino-5-hydroxy-5-polyfluoroalkylcyclohex-2-en-1-ones. *Organic and Biomolecular Chemistry*, *17*(17), 4273–4280. https://doi.org/10.1039/c9ob00293f

Gu, J., Ma, C., Li, Q. Z., Du, W., & Chen, Y. C. (2014). β,γ-regioselective inverse-electron-demand aza-Diels?Alder reactions with α,β-unsaturated aldehydes via dienamine catalysis. *Organic Letters*, *16*(15), 3986–3989. https://doi.org/10.1021/ol501814p

Gujral, S. S., & Popli, A. (2013). Introduction To Diels Alder Reaction, Its Mechanism And Recent Advantages: A Review. *Indo American Journal of Pharmacutical Research*, *3*(4), 3192–3215. http://www.researchgate.net/publication/ 259042153_ Introduction_ To_Diels_Alder_Reaction_Its_Mechanism_And_Recent_Advantages_A_Review/file/50 463529cc452a3c8a.pdf

Han, B., He, Z. Q., Li, J. L., Li, R., Jiang, K., Liu, T. Y., & Chen, Y. C. (2009). Organocatalytic regio- and stereoselective inverse-electron-demand aza-diels-alder reaction of α, β-unsaturated aldehydes and n-tosyl-1-aza-1, 3-butadienes. *Angewandte Chemie - International Edition*, *48*(30), 5474–5477. https://doi.org/10.1002/ anie.200902216

Harutyunyan, A. A. (2016). Condensation of pyrido[1,2-a]pyrimidine with aromatic aldehydes. Synthesis of fused polycyclic pyrimidines. *Russian Journal of Organic Chemistry*, *52*(6), 916–917. https://doi.org/10.1134/S1070428016060294

Hashimoto, Y., Abe, R., Morita, N., & Tamura, O. (2018). Inverse-electron-demand Diels-Alder reactions of α,β-unsaturated hydrazones with 3-methoxycarbonyl α-pyrones. *Organic and Biomolecular Chemistry*, *16*(46), 8913–8916. https://doi.org/10.1039/c8ob02132e

Hashimoto, Y., Ikeda, T., Ida, A., Morita, N., & Tamura, O. (2019). Inverse-Electron-Demand oxa-Diels-Alder Reactions of α-Keto-β,γ-unsaturated Esters and α,β-Unsaturated Hydrazones. *Organic Letters*, *21*(11), 4245–4249. https://doi.org/10.1021/acs.orglett.9b01422

Hatano, M., Sakamoto, T., Mochizuki, T., & Ishihara, K. (2019). Tris(pentafluorophenyl)borane-Assisted Chiral Phosphoric Acid Catalysts for Enantioselective Inverse-Electron-Demand Hetero-Diels-Alder Reaction of α,β-Substituted Acroleins. *Asian Journal of Organic Chemistry*, *8*(7), 1061–1066. https://doi.org/10.1002/ajoc.201900104

Hejmanowska, J., Jasiński, M., Wojciechowski, J., Mlostoń, G., & Albrecht, Ł. (2017). The first organocatalytic,: Ortho -regioselective inverse-electron-demand hetero-Diels-Alder reaction. *Chemical Communications*, *53*(83), 11472–11475. https://doi.org/10.1039/c7cc06518c

Huang, G., Guillot, R., Kouklovsky, C., Maryasin, B., & de la Torre, A. (2022). Diastereo- and Enantioselective Inverse-Electron-Demand Diels–Alder Cycloaddition between 2-Pyrones and Acyclic Enol Ethers. *Angewandte Chemie*, *134*(42). https://doi.org/10.1002/ange.202208185

Inukai, T., & Kasai, M. (1965). Diels-Alder Reactions of Acrylic Acid Derivatives Catalyzed by Aluminum Chloride. *Journal of Organic Chemistry*, *30*(10), 3567–3569. https://doi.org/10.1021/jo01021a508

Inukai, T., & Kojima, T. (1967). Aluminum Chloride Catalyzed Diene Condensation. III.1, 2 Reaction of trans-piperylene with Methyl Acrylate. *Journal of Organic Chemistry*, *32*(4), 869–871. https://doi.org/10.1021/jo01279a003

Jędrzejewski, B., Musiejuk, M., Doroszuk, J., & Witt, D. (2021). Convenient synthesis of functionalized unsymmetrical vinyl disulfides and their inverse electron-demand hetero-diels-alder reaction. *Materials*, *14*(6). https://doi.org/10.3390/ma14061342

Jiang, X., Zhu, H., Shi, X., Zhong, Y., Li, Y., & Wang, R. (2013). Heterogeneous bifunctional catalytic, chemo-, regio- and enantioselective cascade inverse electron demand Diels-Alder reaction. *Advanced Synthesis and Catalysis*, *355*(2–3), 308–314. https://doi.org/10.1002/adsc.201201038

Jouha, J., Buttard, F., Lorion, M., Berthonneau, C., Khouili, M., Hiebel, M. A., Guillaumet, G., Brière, J. F., & Suzenet, F. (2017). Domino Aza-Michael-ih-Diels-Alder Reaction to Various 3-Vinyl-1,2,4-triazines: Access to Polysubstituted Tetrahydro-1,6-naphthyridines. *Organic Letters*, *19*(18), 4770–4773. https://doi.org/ 10.1021/acs.orglett.7b02132

Kai-Xuan, Y., Dong-Sheng, J., Haixue, Z., Yucheng, G., and Peng-Fei, X. (2022). Organocatalytic inverse-electron-demand Diels–Alder reaction between 5-alkenyl thiazolones and β,γ-unsaturated carbonyl compounds. *Chemical Communnication.* 58, 4227-4230

K. N. Houk and R. W. Strozier. (1973). Lewis acid catalysis of Diels-Alder reactions. *J. Am. Chem. Soc.*, *95*(12), 4094–4096. https://doi.org/https://doi.org/10.1021/ja00793a070

Kessler, S. N., & Wegner, H. A. (2010). Lewis acid catalyzed inverse electron-demand diels-alder reaction of 1,2-diazines. *Organic Letters*, *12*(18), 4062–4065. https://doi.org/10.1021/ol101701z

Kim, C. E., Son, J. Y., Shin, S., Seo, B., & Lee, P. H. (2015). Alkenylation of phosphacoumarins via aerobic oxidative heck reactions and their synthetic application to fluorescent benzophosphacoumarins. *Organic Letters*, *17*(4), 908–911. https://doi.org/10.1021/acs.orglett.5b00020

Knall, A. C., Hollauf, M., & Slugovc, C. (2014). Kinetic studies of inverse electron demand Diels-Alder reactions (iEDDA) of norbornenes and 3,6-dipyridin-2-yl-1,2,4,5-tetrazine. *Tetrahedron Letters*, *55*(34), 4763–4766. https://doi.org/10.1016/j.tetlet.2014.07.002

Lai, S., Mao, W., Song, H., Xia, L., & Xie, H. (2016). A biocompatible inverse electron demand Diels-Alder reaction of aldehyde and tetrazine promoted by proline. *New Journal of Chemistry*, *40*(10), 8194–8197. https://doi.org/10.1039/c6nj01567k

Laina-Martín, V., Fernández-Salas, J. A., & Alemán, J. (2021). Organocatalytic Strategies for the Development of the Enantioselective Inverse-electron-demand Hetero-Diels-Alder Reaction. *Chemistry - A European Journal*, *27*(49), 12509–12520. https://doi.org/10.1002/chem.202101696

Lauberteaux, J., Lebrun, A., Van Der Lee, A., Mauduit, M., Marcia De Figueiredo, R., & Campagne, J. M. (2019). Iron-Catalyzed Enantioselective Intramolecular Inverse Electron-Demand Hetero Diels-Alder Reactions: An Access to Bicyclic Dihydropyran Derivatives. *Organic Letters*, *21*(24), 10007–10012. https://doi.org/10.1021/acs.orglett.9b03752

Levandowski, B. J., Abularrage, N. S., Houk, K. N., & Raines, R. T. (2019). Hyperconjugative Antiaromaticity Activates 4 H-Pyrazoles as Inverse-Electron-Demand Diels-Alder Dienes. *Organic Letters*, *21*(20), 8492–8495. https://doi.org/10.1021/acs.orglett.9b03351

Li, W., Yang, N., & Lv, Y. (2015). Theoretical study of the BINOL-zinc complex-catalyzed asymmetric inverse-electron-demand imino Diels-Alder reaction: Mechanism and stereochemistry. *RSC Advances*, *5*(113), 93318–93330. https://doi.org/10.1039/c5ra17981e

Li, Y., Hu, Y., Zhang, S., Sun, J., Li, L., Zha, Z., & Wang, Z. (2016). Copper-Catalyzed Enantioselective Hetero-Diels-Alder Reaction of Danishefsky's Diene with Glyoxals. *Journal of Organic Chemistry*, *81*(7), 2993–2999. https://doi.org/10.1021/acs.joc.5b02780

Liang, X. W., Zhao, Y., Si, X. G., Xu, M. M., Tan, J. H., Zhang, Z. M., Zheng, C. G., Zheng, C., & Cai, Q. (2019). Enantioselective Synthesis of Arene cis-Dihydrodiols from 2-Pyrones. *Angewandte Chemie - International Edition*, *58*(41), 14562–14567. https://doi.org/10.1002/anie.201908284

Lorion, M., Guillaumet, G., Brière, J. F., & Suzenet, F. (2015). Sequential Michael Addition and Enamine-Promoted Inverse Electron Demanding Diels-Alder Reaction upon 3-Vinyl-1,2,4-triazine Platforms. *Organic Letters*, *17*(12), 3154–3157. https://doi.org/10.1021/acs.orglett.5b01487

Macias-Contreras, M., He, H., He, H., Little, K. N., Lee, J. P., Campbell, R. P., Royzen, M., Zhu, L., & Zhu, L. (2020). SNAP/CLIP-Tags and Strain-Promoted Azide-Alkyne Cycloaddition (SPAAC)/Inverse Electron Demand Diels-Alder (IEDDA) for Intracellular Orthogonal/Bioorthogonal Labeling. *Bioconjugate Chemistry*, *31*(5), 1370–1381. https://doi.org/10.1021/acs.bioconjchem.0c00107

Maity, R., & Pan, S. C. (2017). Dienamine-Mediated Asymmetric Inverse-Electron-Demand Hetero-Diels–Alder Reaction of Linear Deconjugated Enones: Diversity-Oriented Synthesis of 3,4-Dihydropyrans. *European Journal of Organic Chemistry*, *2017*(4), 871–874. https://doi.org/10.1002/ejoc.201601575

Mansot, J., Lauberteaux, J., Lebrun, A., Mauduit, M., Vasseur, J. J., Marcia de Figueiredo, R., Arseniyadis, S., Campagne, J. M., & Smietana, M. (2020). DNA-Based Asymmetric Inverse Electron-Demand Hetero-Diels–Alder. *Chemistry - A European Journal*, *26*(16), 3519–3523. https://doi.org/10.1002/chem.202000516

Martin, R. E., Lenz, M., Alzieu, T., Aebi, J. D., & Forzy, L. (2013). Flow synthesis of annulated 5-aryl-substituted pyridines by tandem intramolecular inverse-electron-demand hetero-/retro-Diels-Alder reaction. *Tetrahedron Letters*, *54*(49), 6703–6707. https://doi.org/10.1016/j.tetlet.2013.09.069

Meltzer, H. Y., Simonovic, M., & Gudelsky, G. A. (1983). Effects of pirenperone and ketanserin on rat prolactin secretion in vivo and in vitro. *European Journal of Pharmacology*, *92*(1–2), 83–89. https://doi.org/10.1016/0014-2999(83)90111-5

Mrug, G. P., Kondratyuk, K. M., Bondarenko, S. P., & Frasinyuk, M. S. (2016). Inverse electron demand Diels–Alder reactions with aminomethyl derivatives of 3-arylhydroxycoumarins. *Chemistry of Heterocyclic Compounds*, *52*(7), 460–466. https://doi.org/10.1007/s10593-016-1907-6

Mubofu, E. B., & Engberts, J. B. F. N. (2004). Specific acid catalysis and Lewis acid catalysis of Diels-Alder reactions in aqueous media. *Journal of Physical Organic Chemistry*, *17*(3), 180–186. https://doi.org/10.1002/poc.711

N. R. Campbell and J. H. Hunt. (1947). ?=r : : 8. *J. Am. Chem. Soc.*, *2*(1176), 1176–1179.

Narayan, V., Mishra, H. N., Prasad, O., & Sinha, L. (2011). Electronic structure, electric moments and vibrational analysis of 5-nitro-2-furaldehyde semicarbazone: A D.F.T. study. *Computational and Theoretical Chemistry*, *973*(1–3), 20–27. https://doi.org/10.1016/j.comptc.2011.06.023

Nellinger, S., Rapp, M. A., Southan, A., Wittmann, V., & Kluger, P. J. (2022). An Advanced 'clickECM' That Can be Modified by the Inverse-Electron-Demand Diels-Alder Reaction. *ChemBioChem*, *23*(1), 1–9. https://doi.org/10.1002/cbic.202100266

Nguyen, K. M. H., Schwendimann, L., Gressens, P., & Largeron, M. (2015). Regiospecific synthesis of neuroprotective 1,4-benzoxazine derivatives through a tandem oxidation-Diels-Alder reaction. *Organic and Biomolecular Chemistry*, *13*(12), 3749–3756. https://doi.org/10.1039/c5ob00049a

Novianti, I., Kowada, T., & Mizukami, S. (2022). Clip to Click: Controlling Inverse Electron-Demand Diels-Alder Reactions with Macrocyclic Tetrazines. *Organic Letters*, *24*(17), 3223–3226. https://doi.org/10.1021/acs.orglett.2c01010

Nwagbara, A. J. (2015). *Inverse Electron Demand Diels - Alder Chemistry of Electron Deficient Chromone - fused Dienes By*. *October*.

Pałasz, A., Kalinowska-Tłuścik, J., & Jabłoński, M. (2013). Application of 2,4,6-trioxo-pyrimidin-5-ylidene alditols in the synthesis of pyrano[2,3-d]pyrimidines containing a sugar moiety by hetero-Diels-Alder reactions and by conjugate Michael addition-cyclizations. *Tetrahedron*, *69*(38), 8216–8227. https://doi.org/10.1016/j.tet.2013.07.032

Pałasz, A., & Pałasz, T. (2011). Knoevenagel condensation of cyclic ketones with benzoylacetonitrile and N,N′-dimethylbarbituric acid. Application of sterically hindered condensation products in the synthesis of spiro and dispiropyrans by hetero-Diels-Alder reactions. *Tetrahedron*, *67*(7), 1422–1431. https://doi.org/10.1016/j.tet.2010.12.053

Park, K. H. K., Frank, N., Duarte, F., & Anderson, E. A. (2022). Collective Synthesis of Illudalane Sesquiterpenes via Cascade Inverse Electron Demand (4 + 2) Cycloadditions of Thiophene S, S-Dioxides. *Journal of the American Chemical Society*, *144*(22), 10017–10024. https://doi.org/10.1021/jacs.2c03304

Peter Yates and Philip Eaton. (1960). h 1 : 1. *Journal of the American Chemical Society*, *82*(ii), 4436–4437. https://doi.org/10.1021/ja01501a085

Philosophie, D. Der, & Kessler, S. N. (2013). *Development of a Bidentate Lewis Acid Catalyzed Inverse Electron Demand Diels-Alder Reaction of 1 , 2-Diazines for the Synthesis of Substituted Arenes*.

Png, Z. M., Zeng, H., Ye, Q., & Xu, J. (2017). Inverse-Electron-Demand Diels–Alder Reactions: Principles and Applications. *Chemistry - An Asian Journal*, *12*(17), 2142–2159. https://doi.org/10.1002/asia.201700442

Pottie, I. R., Nandaluru, P. R., Benoit, W. L., Miller, D. O., Dawe, L. N., & Bodwell, G. J. (2011). Synthesis of 6 H-dibenzo[b, d]pyran-6-ones using the inverse electron demand Diels-Alder reaction. *Journal of Organic Chemistry*, *76*(21), 9015–9030. https://doi.org/10.1021/jo201775e

Prajapati, D., & Gohain, M. (2006). An efficient synthesis of novel pyrano[2,3-d]- and furopyrano[2,3-d] pyrimidines via indium-catalyzed multi-component domino reaction. *Beilstein Journal of Organic Chemistry*, *2*, 3–7. https://doi.org/10.1186/1860-5397-2-11

Prasad, H. S. N., Ananda, A. P., Lohith, T. N., Prabhuprasad, P., Jayanth, H. S., Krishnamurthy, N. B., Sridhar, M. A., Mallesha, L., & Mallu, P. (2022). Design, synthesis, molecular docking and DFT computational insight on the structure of Piperazine sulfynol derivatives as a new antibacterial contender against superbugs MRSA. *Journal of Molecular Structure*, *1247*, 131333. https://doi.org/10.1016/j.molstruc.2021.131333

Ramesh, E., Sree Vidhya, T. K., & Raghunathan, R. (2008). Indium chloride/silica gel supported synthesis of pyrano/thiopyranoquinolines through intramolecular imino Diels-Alder reaction using microwave irradiation. *Tetrahedron Letters*, *49*(17), 2810–2814. https://doi.org/10.1016/j.tetlet.2008.02.128

Rezvanian, A., Alinaghian, F., & Heravi, M. M. (2018). Metal-Free Assemblage of Four C−N and Two C−C Bonds via a Cascade Five Component Diastereoselective Synthesis of Pyrido[1,2-a]Pyrimidines. *ChemistrySelect*, *3*(41), 11565–11568. https://doi.org/10.1002/slct.201802481

Ruhl, J., Ahles, S., Strauss, M. A., Leonhardt, C. M., & Wegner, H. A. (2021). Synthesis of Medium-Sized Carbocycles via a Bidentate Lewis Acid-Catalyzed Inverse Electron-Demand Diels-Alder Reaction Followed by Photoinduced Ring-Opening. *Organic Letters*, *23*(6), 2089–2093. https://doi.org/10.1021/acs.orglett.1c00249

Saktura, M., Joachim, B., Grzelak, P., & Albrecht, Ł. (2019). Aromatizative Inverse-Electron-Demand Hetero-Diels-Alder Reaction in the Synthesis of Benzothiophene Derivatives. *European Journal of Organic Chemistry*, *2019*(39), 6592–6596. https://doi.org/10.1002/ejoc.201900884

Samba, W. K., Tia, R., & Adei, E. (2021). Regio-, enantio-, peri-, and stereo-selectivities of the reactions of five-membered cyclodiene derivatives with itaconic anhydride toward the formation of norbornene lactones. *Journal of Physical Organic Chemistry*, *34*(2), 1–16. https://doi.org/10.1002/poc.4132

Sanap, K. K., & Samant, S. D. (2015). Regiospecific inverse electron demand Diels-Alder reactions of 7-methylcoumarin-4-azadienes. *RSC Advances*, *5*(46), 36696–36706. https://doi.org/10.1039/c5ra06262d

Schnell, S. D., González, J. A., Sklyaruk, J., Linden, A., & Gademann, K. (2021). Boron Trifluoride-Mediated Cycloaddition of 3-Bromotetrazine and Silyl Enol Ethers: Synthesis of 3-Bromo-pyridazines. *Journal of Organic Chemistry*, *86*(17), 12008–12023. https://doi.org/10.1021/acs.joc.1c01384

Schoch, J., Ameta, S., & Jäschke, A. (2011). Inverse electron-demand Diels-Alder reactions for the selective and efficient labeling of RNA. *Chemical Communications*, *47*(46), 12536–12537. https://doi.org/10.1039/c1cc15476a

Schoch, J., Wiessler, M., & Jäschke, A. (2010). Post-synthetic modification of DNA by inverse-electron-demand diels-alder reaction. *Journal of the American Chemical Society*, *132*(26), 8846–8847. https://doi.org/10.1021/ja102871p

Sharma, P., Kumar, A., Sahu, V., & Singh, J. (2008). Frontier orbital interactions in the hetero Diels-Alder cycloaddition of diazadienes. *Canadian Journal of Chemistry*, *86*(5), 384–394. https://doi.org/10.1139/V08-035

Shen, L. W., Li, T. T., You, Y., Zhao, J. Q., Wang, Z. H., & Yuan, W. C. (2021). Inverse Electron-Demand Aza-Diels-Alder Reaction of Cyclic Enamides with 1,2-Diaza-1,3-dienes in Situ Generated from α-Halogeno Hydrazones: Access to Fused Polycyclic Tetrahydropyridazine Derivatives. *Journal of Organic Chemistry*, *86*(17), 11472–11481. https://doi.org/10.1021/acs.joc.1c00993

Shi, M. L., Zhan, G., Zhou, S. L., Du, W., & Chen, Y. C. (2016). Asymmetric Inverse-Electron-Demand Oxa-Diels-Alder Reaction of Allylic Ketones through Dienamine Catalysis. *Organic Letters*, *18*(24), 6480–6483. https://doi.org/10.1021/acs.orglett.6b03384

Si, X. G., Zhang, Z. M., & Cai, Q. (2021). Asymmetric Inverse-Electron-Demand Diels-Alder Reactions of 2-Pyrones by Lewis Acid Catalysis. *Synlett*, *32*(10), 947–954. https://doi.org/10.1055/a-1371-4391

Sihan, Z., Shaobing, Cheng, H.L., Jiayan, Z., Min, L., Weicheng, Y., & Xiaomei. (2020). Synthesis of chiral [2,3]-fused indolines through enantioselective dearomatization inverse-electron-demand Diels–Alder reaction/oxidation of indoles with 2-(2-nitrovinyl)-1,4-benzoquinone. *The Royal Society of Chemistry,* 56 (60).

Stefano Forli, Ruth Huey, Michael E Pique, Michel F Sanner, D. S. G. & A. J. O. (2016). Low-dielectric-constant polyimide aerogel composite films with low water uptake. *Polymer Journal*, *48*(7), 829–834. https://doi.org/10.1038/pj.2016.37

Stepanova, E. E., & Maslivets, A. N. (2015). [4+2]-Cycloaddition of butyl vinyl ether to 3-aroylpyrrolo[1,2-a]quinoxaline-1,2,4(5H)-triones. *Russian Journal of Organic Chemistry*, *51*(7), 1052–1053. https://doi.org/10.1134/S1070428015070325

Strauss, M. A., Kohrs, D., Ruhl, J., & Wegner, H. A. (2021). Mechanistic Study of Domino Processes Involving the Bidentate Lewis Acid Catalyzed Inverse Electron-Demand Diels−Alder Reaction. *European Journal of Organic Chemistry*, *2021*(28), 3866–3873. https://doi.org/10.1002/ejoc.202100486

Tamilmani, V., Daul, C. A., & Venuvanalingam, P. (2005). Electrostatic control on endo/exo selectivity in ionic cycloaddition. *Chemical Physics Letters*, *416*(4–6), 354–357. https://doi.org/10.1016/j.cplett.2005.09.120

Tanaka, K., Kishimoto, M., Asada, Y., Tanaka, Y., Hoshino, Y., & Honda, K. (2019). Access to Electron-Deficient 2,2-Disubstituted Chromanes: A Highly Regioselective One-Pot Synthesis via an Inverse-Electron-Demand [4 + 2] Cycloaddition of ortho-Quinone Methides. *Journal of Organic Chemistry*, *84*(21), 13858–13870. https://doi.org/10.1021/acs.joc.9b02036

Taotao, C., Chao, C., Zhefei, G., Xiu-Qin D., & Chun-Jiang W. (2021) Diastereoselective synthesis of functionalized tetrahydropyridazines containing indole scaffolds via an inverse-electron-demand aza-Diels–Alder reaction. *Organic Chemistry Front*iers, 8, 4392

Tingting, Z., Anquan, Z., Luqiong, H., Changgeng, L., Haibo, T., Sasa W., & Huiyu, C. (2022). Total syntheses of ericifolione and its analogues *via* a biomimetic inverse-electron-demand Diels–Alder reaction. Chemical Communnicati*on,* ,58, 270-273.

Tirado-Rives, J., & Jorgensen, W. L. (2008). Performance of B3LYP density functional methods for a large set of organic molecules. *Journal of Chemical Theory and Computation*, *4*(2), 297–306. https://doi.org/10.1021/ct700248k

Toche, R. B., Ghotekar, B. K., Kazi, M. A., Patil, S. P., & Jachak, M. N. (2008). New Approach for the Synthesis of Pyrido[1,2-a]pyrimidines. *Scholarly Research Exchange*, *2008*, 1–5. https://doi.org/10.3814/2008/434329

Tong, M. C., Chen, X., Li, J., Huang, R., Tao, H., & Wang, C. J. (2014). Catalytic asymmetric synthesis of [2,3]-fused indoline heterocycles through inverse-electron-demand aza-Diels-Alder reaction of indoles with azoalkenes. *Angewandte Chemie - International Edition*, *53*(18), 4680–4684. https://doi.org/10.1002/anie.201400109

Tormena, C. F., Lacerda, V., & De Oliveg, K. T. (2010). Revisiting the stability of endo/exo diels-alder adducts between cyclopentadiene and 1,4-benzoquinone. *Journal of the Brazilian Chemical Society*, *21*(1), 112–118. https://doi.org/10.1590/S0103-50532010000100017

Türkmen, Y. E., Montavon, T. J., Kozmin, S. A., & Rawal, V. H. (2012). Silver-catalyzed formal inverse electron-demand diels-alder reaction of 1,2-diazines and siloxy alkynes. *Journal of the American Chemical Society*, *134*(22), 9062–9065. https://doi.org/10.1021/ja302537j

Venugopal, S., & Sundaram, S. (2016). *Simple and Ef fi cient Synthesis of 2-Oxo-2H-Pyrido [1 , 2-a] Pyrimidin-3 (4H) - Ylidene Acetic Acid and Its Rearrangement in Presence of Acid Media*. *3*(i), 882–886. https://doi.org/10.1002/jhet

Verma, A. K., Bishnoi, A., Fatma, S., Parveen, H., & Singh, V. (2017). An Easy Synthetic Access to Spiro Derivatives Containing Pyrido[1,2-a]pyrimidine and Quinoline Scaffolds and Their Antimicrobial Activity. *ChemistrySelect*, *2*(14), 4006–4009. https://doi.org/10.1002/slct.201700228

Vicario, J., Aparicio, D., & Palacios, F. (2011). A diastereoselective aza-Diels-Alder reaction of N-aryl-1-azadienes derived from α-amino acids with enamines. *Tetrahedron Letters*, *52*(32), 4109–4111. https://doi.org/10.1016/j.tetlet.2011.05.119

Vuong, H., Dash, B. P., Nilsson Lill, S. O., & Klumpp, D. A. (2018). Diels-Alder Reactions with Ethylene and Superelectrophiles. *Organic Letters*, *20*(7), 1849–1852. https://doi.org/10.1021/acs.orglett.8b00367

Wang, S. W., Guo, W. S., Wen, L. R., & Li, M. (2014). A new approach to pyridines through the reactions of methyl ketones with 1,2,4-triazines. *RSC Advances*, *4*(103), 59218–59220. https://doi.org/10.1039/c4ra11294f

Wappl, C., Schallert, V., Slugovc, C., Knall, A. C., & Spirk, S. (2021). Highly norbornylated cellulose and its "Click" modification by an inverse-electron demand diels-alder (iEDDA) reaction. *Molecules*, *26*(5), 1–12. https://doi.org/10.3390/molecules26051358

Wei, L., Zhu, Q., Song, Z. M., Liu, K., & Wang, C. J. (2018). Catalytic asymmetric inverse electron demand Diels-Alder reaction of fulvenes with azoalkenes. *Chemical Communications*, *54*(20), 2506–2509. https://doi.org/10.1039/c7cc09896k

Weise, C. F., Lauridsen, V. H., Rambo, R. S., Iversen, E. H., Olsen, M. L., & Jørgensen, K. A. (2014). Organocatalytic access to enantioenriched dihydropyran phosphonates via an inverse-electron-demand hetero-Diels-Alder reaction. *Journal of Organic Chemistry*, *79*(8), 3537–3546. https://doi.org/10.1021/jo500347a

Wittmann, B. M., Stirdivant, S. M., Mitchell, M. W., Wulff, J. E., McDunn, J. E., Li, Z., Dennis-Barrie, A., Neri, B. P., Milburn, M. V., Lotan, Y., & Wolfert, R. L. (2014). Bladder cancer biomarker discovery using global metabolomic profiling of urine. *PLoS ONE*, *9*(12), 1–19. https://doi.org/10.1371/journal.pone.0115870

Xu, Z., Liu, L., Wheeler, K., & Wang, H. (2011). Asymmetric inverse-electron-demand hetero-Diels-Alder reaction of six-membered cyclic ketones: An enamine/metal lewis acid bifunctional approach. *Angewandte Chemie - International Edition*, *50*(15), 3484–3488. https://doi.org/10.1002/anie.201100160

Yanagihara, Y., Kasap, H., Kawashima, T., Shida, T., & Kawashima, T. (1988). Immunopharmacological Studies on TBX, a New Antiallergic Drug (1) Inhibitory Effects on Passive Cutaneous Anaphylaxis in Rats and Guinea Pigs. *Japanese Journal of Pharmacology*, *48*(1), 91–101. https://doi.org/10.1254/jjp.48.91

Yang, B., & Kwon, I. (2021). Multivalent Albumin-Neonatal Fc Receptor Interactions Mediate a Prominent Extension of the Serum Half-Life of a Therapeutic Protein. *Molecular Pharmaceutics*, *18*(6), 2397–2405. https://doi.org/10.1021/acs.molpharmaceut.1c00231

Yang, K., Dang, Q., Cai, P. J., Gao, Y., Yu, Z. X., & Bai, X. (2017). Reaction of Aldehydes/Ketones with Electron-Deficient 1,3,5-Triazines Leading to Functionalized Pyrimidines as Diels-Alder/Retro-Diels-Alder Reaction Products: Reaction Development and Mechanistic Studies. *Journal of Organic Chemistry*, *82*(5), 2336–2344. https://doi.org/10.1021/acs.joc.6b02570

Yang, L., ,Meng-Meng, Xu,Zhi-Mao., Zhang., ,Prof. Dr. Junliang., & Z., Prof. Dr. Quan, C. (2021). Catalytic Asymmetric Inverse-Electron-Demand Diels–Alder Reactions of 2-Pyrones with Indenes: Total Syntheses of Cephanolides A and B. 60 (51) ,26610-26615.

Yang, W., Zhou, Z., Zhao, Y., Luo, D., Luo, X., Luo, H., Cui, L., & Li, L. (2022). Copper Catalyzed Inverse Electron Demand [4+2] Cycloaddition for the Synthesis of Oxazines. *Catalysts*, *12*(5). https://doi.org/10.3390/catal12050526

Yang, Y. F., Yu, P., & Houk, K. N. (2017). Computational Exploration of Concerted and Zwitterionic Mechanisms of Diels-Alder Reactions between 1,2,3-Triazines and Enamines and Acceleration by Hydrogen-Bonding Solvents. *Journal of the American Chemical Society*, *139*(50), 18213–18221. https://doi.org/10.1021/jacs.7b08325

Ye, Q., Neo, W. T., Cho, C. M., Yang, S. W., Lin, T., Zhou, H., Yan, H., Lu, X., Chi, C., & Xu, J. (2014). Synthesis of ultrahighly electron-deficient pyrrolo[3,4- d]pyridazine-5,7-dione by inverse electron demand diels-alder reaction and its application as electrochromic materials. *Organic Letters*, *16*(24), 6386–6389. https://doi.org/10.1021/ol503178m

Yu, P., Li, W., & Houk, K. N. (2017). Mechanisms and Origins of Selectivities of the Lewis Acid-Catalyzed Diels-Alder Reactions between Arylallenes and Acrylates. *Journal of Organic Chemistry*, *82*(12), 6398–6402. https://doi.org/10.1021/acs.joc.7b01132

Zhang, F., Ren, B. T., Zhou, Y., Liu, Y., & Feng, X. (2022). Enantioselective construction of cis-hydroindole scaffolds via an asymmetric inverse-electron-demand Diels-Alder reaction: application to the formal total synthesis of (+)-minovincine. *Chemical Science*, 5562–5567. https://doi.org/10.1039/d2sc01458k

Zhang, J., Shukla, V., & Boger, D. L. (2019). Inverse Electron Demand Diels-Alder Reactions of Heterocyclic Azadienes, 1-Aza-1,3-Butadienes, Cyclopropenone Ketals, and Related Systems. A Retrospective. *Journal of Organic Chemistry*, *84*(15), 9397–9445. https://doi.org/10.1021/acs.joc.9b00834

Zhang, Z., Jamieson, C. S., Zhao, Y. L., Li, D., Ohashi, M., Houk, K. N., & Tang, Y. (2019). Enzyme-Catalyzed Inverse-Electron Demand Diels-Alder Reaction in the Biosynthesis of Antifungal Ilicicolin H. *Journal of the American Chemical Society*, *141*(14), 5659–5663. https://doi.org/10.1021/jacs.9b02204

Zhao, Z., Dai, X., Li, C., Wang, X., Tian, J., Feng, Y., & Xie, J. (2020). *Pyrazolone structural motif in medicinal chemistry : Retrospect and prospect*. *186*(January).

Zhou, Y., Zhu, Y., Lin, L., Zhang, Y., Zheng, J., Liu, X., & Feng, X. (2014). N,N′-Dioxide/Nickel(II)-Catalyzed Asymmetric Inverse-Electron-Demand Hetero-Diels-Alder Reaction of β,γ-Unsaturated α-Ketoesters with Enecarbamates. *Chemistry - A European Journal*, *20*(50), 16753–16758. https://doi.org/10.1002/chem.201403764

Zhu, Y., Chen, X., Xie, M., Dong, S., Qiao, Z., Lin, L., Liu, X., & Feng, X. (2010). Asymmetric diels-alder and inverse-electron-demand hetero-Diels-Alder reactions of β,γ-unsaturated α-ketoesters with cyclopentadiene catalyzed by N,N′-dioxide copper(II) complex. *Chemistry - A European Journal*, *16*(39), 11963–11968. https://doi.org/10.1002/chem.201001365

Appendices

Appendix-1

COMPUTATIONAL DETAILS

Frontier molecular orbitals (FMOs)

The optical and electrical characteristics of organic molecules are widely described via FMO analysis. When two molecules interact, the energy of the HOMO (electronic donors) is related to the ionisation potential (IP-Equation 1) and the energy of the LUMO (electronic acceptors) is related to the electron affinity (EA-Equation 2).The final charge transfer interaction within the molecule is explained by the HOMO-LUMO energy gap (Equation 3) which aids in determining the molecular electrical transport features. Electronic chemical potential (μ), chemical hardness (η), global electrophilities (ω), and maximum charge transfer (ΔN_{max}) were estimated as global reactivity indices.

Equations 7 and 8 were also used to compute global electrophilicities ω and ΔN_{max}. The electrophilicity index, which assesses a reaction substrate's capacity to receive electrons, has been used to analyse chemical reactivities.

Ionization potential (IP) = $-E_{HOMO}$ ..... **(1)**

Electron Affinity (EA) = $- E_{LUMO}$ ..... **(2)**

$E_{gap} = (E_{LUMO} - E_{HOMO})$ .....**(3)**

Chemicalpotential(μ) = $(E_{HOMO} + E_{LUMO})/2$ ..... **(4)**

Chemicalhardness (η) = $(E_{LUMO} - E_{HOMO})$ ..... **(5)**

Chemical softness (σ) = $1/ 2\eta$ ..... **(6)**

Electrophilicity index (ω) = $\mu^2/2\eta$ ..... **(7)**

$\Delta N_{max} = - \mu/\eta$ ..... **(8)**

Thermodynamic Properties

The ground state energy and the statistically mechanically determined data were combined Eq. 9 to 14.

i. Enthalpy(H)

Sum of electronic and thermal enthalpies (H) = $E_0 + H_{corr}$ **..... (9)**

Where: E_0- the total electronic energy, H_{corr} - correction to the enthalpy due to internal energy, H – enthalpy of the species

$$\Delta H_{Rxn} = (E_0 + H_{corr})\ \text{product} - (E_0 + H_{corr})\ \text{reactant at (298K)} \quad \textbf{..... (10)}$$

Where: ΔHrxn - change in enthalpy of reaction; E_0- the total electronic energy of reactants and products and H_{corr} - correction to the enthalpy due to internal energy of reactants and products.

ii. **Activation energy (E_a)** was calculated Eq. [3]:

$$E_a = \Delta H + RT \quad \textbf{..... (11)}$$

Where: Ea - activation energy, ΔH - change in enthalpy, R - gas constant and T – temperature (298K).

iii. The **entropy of the reaction** was calculated by subtracting the entropies of the reactant and product, which is given by Eq[12]

$$\Delta S_{reaction} = S_{product} - S_{reactants} \quad \textbf{..... (12)}$$

Where: S - entropy and ΔS - change in entropy.

iv. The **Gibbs free energy** of activation was calculated and computed using the heat of reaction equation's modified form. Understanding that Eq. [13].

Sum of electronic and thermal free energies = $E_0 + G_{corr}$

Where: G_{corr} - correction to the Gibbs free energy due to internal energy

$$G = H - TS \quad \textbf{..... (13)}$$

$$\Delta G = \Delta H - T\Delta S \quad \textbf{..... (14)}$$

ANTIBACTERIAL SUSCEPTIBILITY TESTING (Kirby-Bauer method)

Objective

Determine the susceptibility of two bacterial species to various samples.

Procedure

The growth method was performed as follows

1. At least three to five well-isolated colonies of the same morphological type were selected from agar plate culture. The top of each colony was touched with a loop, and the growth was transferred to a tube containing 4 to 5 ml of an appropriate culture medium, such as Müeller-Hinton broth.

2. The broth culture was incubated at 35°C until it achieves or exceeds the turbidity (usually 2 to 6 hours)

3. The turbidity of the actively growing broth culture was adjusted with sterile saline or broth to obtain a turbidity. This resulted in a suspension containing approximately 1 to 2 x 10^8 CFU/ml for *Escherichia coli and Staphylococccus aureus.*

Inoculation of Test Plates

1. Optimally, within 15 minutes after adjusting the turbidity of the inoculum suspension, a sterile cotton swab was dipped into the adjusted suspension. The swab should be rotated several times and pressed firmly on the inside wall of the tube above the fluid level. This will remove excess inoculum from the swab.
2. The dried surface of a Müeller-Hinton agar plate is inoculated by streaking the swab over the entire sterile agar surface. This procedure is repeated by streaking two more times, rotating the plate approximately 60° each time to ensure an even distribution of inoculum. As a final step, the rim of the agar is swabbed.
3. The lid may be left ajar for 3 to 5 minutes, but no more than 15 minutes, to allow for any excess surface moisture to be absorbed before applying the drug impregnated disks.
4. The media was punctured by making a well of 6 mm in diameter and filled with 50 µl of a sample. Further the Petri plates were placed inversely for complete diffusion and inhibition zones were examined by measuring the diameter (mm) formed around the well after 24 hrs incubation at 37°C. The zones were measured by using standard (Hi-Media) scale.

MOLECULAR DOCKING

Docking tests were performed to see how the synthesised compounds inhibit bacterial growth and to determine the compounds' binding affinity and interactions with different target proteins in *Escherichia coli* and *Staphylococcus aureus*. The docking process is divided into the following steps.

Preparation of ligands and proteins

The structure of synthesised compounds was drawn in ChemDraw Ultra 12.0 and converted to Pdf file format using open babel software. The protein structures were downloaded in PDB format from RCSB Protein Data Bank. Water molecules and ligands initially present in the proteins were removed using Auto Dock tools 1.5.7 software, and hydrogen atoms were inserted and saved in PDB format**.** To assess the interaction with synthesised compounds, two target proteins from *Escherichia coli* and *Staphylococcus aureus* were used.

Target protein in *Staphylococcus aureus*

Dihydrofolate reductase (DHFR) (PDB ID: 2W9S): The enzyme dihydrofolate reductase (DHFR) catalyses the synthesis of tetrahydrofolate (THF) by reducing dihydrofolate (DHF) in the presence of nicotinamide adenine dinucleotide phosphate (NADPH). It is also vital in the synthesis of thymidylate, purines, methionine, and other key metabolites. Cell proliferation requires the presence of these enzymes. Thus, inhibiting dihydrofolate reductase destroys the intracellular tetrahydrofolate pool, blocking the production of RNA, DNA, thymidine, and protein. They are anticancer and antibacterial drugs' targets due to their vast variety of cellular functions**.**

Target protein in *Escherichia coli*

Uridine diphospho-N-Acetylenolpyruvyl Glucosamine Reductase (1MBT) is an essential enzyme that catalyses the reduction of the cell wall precursor's enolpyruvyl uridine diphosphate Nacetyl glucosamine (EPUNAG) to uridine diphosphate Nacetyl muramic acid (UNAM). 1MBT (Mur A, F, Y, and G) catalyses a range of metabolic transformations involved in the production of the peptidoglycan layer of bacterial cell walls, as well as the preservation of several bacterial strains**.**

Docking simulations

Docking calculations were performed using the software Autodock vina 1.5.6, and the binding energy of the protein—Synthesized adducts was determined. Using the graphical interface programme 'MGL tools,' the ligand was then converted into PDBQT. The protein data bank coordinate file with the names 2W9S and 1MBT was used as an antibacterial receptor molecule. To run docking simulations, the grid box was modified with 'MGL tools.' The best docked conformation and binding affinity for drugs with proteins were determined using Autodock Vina**.**

Visualization of protein-ligand complexes

LigPlot+ and PyMol were used to generate a visual representation of the interaction between the ligands and the target protein. Using the 2W9S and 1MBT -Proteins, the 3D coordinates of the target receptor were obtained, and the optimal docked conformation of the examined structures was selected using glide energy, docking score, active hydrogen bonding sites, and hydrophobic interactions. The compound's binding affinity with the target protein is the sum of all the interactions and binding energy that exist between them

LIPINSKI RULE OF FIVE (ADME)

According to the Lipinski rule, an orally active drug should be tiny and mildly lipophilic. This rule shows molecular features rather than pharmacological activity and states that a drug has good oral activity if it meets five parameters, such as the ones listed below

1. Molecular weight < 500
2. Octanol-water partition coefficient log$P$ < 5
3. Less than 5 hydrogen bond donors (total number ofNH and OH bonds)
4. Less than 10 hydrogen bond acceptors (totalnumber of N and O atoms)
5. Molar refractivity between 40 and 130

Asian Journal of Chemistry; Vol. 34, No. 10 (2022), 2623-2632

ASIAN JOURNAL OF CHEMISTRY

https://doi.org/10.14233/ajchem.2022.23865

DFT, Molecular Docking, Toxicity Investigations and Antifungal Efficacy of *N*-Aryl Amides of Pyrido[1,2-*a*]pyrimidin-2-one

ABINAYA ANBAZHAGAN and SHARULATHA VENUGOPAL*

Department of Chemistry, Avinashilingam Institute for Home Science and Higher Education for Women, Coimbatore-641043, India

*Corresponding author: E-mail: sharulatha_chem@avinuty.ac.in

Received: 8 April 2022; *Accepted*: 23 June 2022; *Published online*: 19 September 2022; AJC-20965

Potent kinase inhibitors containing *N*-aryl bonds play a crucial role for enzyme inhibition. Hence, the present investigation was carried out to evaluate the antifungal activity of *N*-aryl amides of pyrido[1,2-*a*]pyrimidin 2-ones. The synthesized compounds were evaluated for their *in vitro* antifungal activity against *Aspergillus niger* and *Candida albicans* by the disc diffusion method. All the compounds showed significant antifungal activity. Further, the docking studies were carried out against the active site of 1NMT and 1KS5 fungi protein. The whole compounds showed great binding affinity and possess bioavailability. DFT/B3LYP technique using the 6-31G basis set at gaseous phase all the compounds were optimized and the HOMO-LUMO energies also calculated. Furthermore, *in silico* prediction of toxicity and bioactive score values indicates that the compounds are highly reactive. According to Lipinski's "rule of five," all the compounds are expected to be biologically active. It is expected that these findings will provide clarity regarding molecular recognition and will undoubtedly aid drug scientists in developing novel drugs in the future.

Keywords: Pyridopyrimidine, Antifungal Activity, Molecular docking, DFT, Toxicity, Molecular properties.

INTRODUCTION

One of medicinal chemistry's greatest achivements has been in the fight against fungal infection. The only medicine available to cure major fungal infections was amphotericin, which is known to cause considerable nephrotoxicity. The approval of imidazoles and triazoles in the late 1980s marked a significant improvement to treat local and systemic fungal infections safely and efficiently [1]. These developments and the associated increase in fungal infections intensified the search for new, safer and more effacious agents to combat serious fungal infections.

Pyridopyrimidine is a fascinating heterocyclic moiety that has high antifungal activity and is made up of a number of physiologically active compounds [2]. The pyridopyrimidine ring's polar nitrogen atom promotes bioactivity to compounds and facilitates their interaction with macromolecules [3]. Its derivatives have long been used in the synthesis of medicinal intermediates. With the various therapeutic properties of the pyridopyrimidine ring in mind, it is decided to synthesize a number of compounds with nitrogen as core element and assays them *in vitro* for antifungal activity [4]. Biological effects of amide derivatives include anticancer, antihistamine, antifungal, and antibacterial activities. Many potent kinase inhibitors containing *N*-aryl bonds play a crucial role for enzyme inhibition as observed in the case of imatinib and ZM-447439 [5].

Designing of drugs for various diseases necessitates theoretical modeling of the drug's structure. Rather than synthesizing the appropriate compounds for treatment, researchers prefer to design the structure of drugs using theoretical modeling. One such method is molecular docking, which involves checking the interaction of drugs with the appropriate proteins [6]. Molecular docking is a computational method for predicting the binding of bioactive compounds to specific proteins or for predicting the target proteins for one bioactive compound [7]. In drug design industry, molecular docking is an effective strategy for gaining insight into ligand-receptor interactions. Molecular docking plays a significant role in drug development due its ability to predict the best binding mode between drugs and the target protein [8].

N-Aryl amides derivatives were synthesized in prior investigations and some of the compounds exhibited potential

antibacterial activity against phytopathogens [9]. In continuation of our research, the current work evaluates the antifungal efficacy of *N*-aryl amides of pyrido[1,2-*a*]pyrimidin 2-ones as well as *in silico* analyses such as molecular docking, DFT, toxicity, bioactive score and ADME property.

EXPERIMENTAL

N-Aryl amides derivatives were synthesized according to the reported procedure [9] and used for the antifungal activity.

Antifungal activity: The disc diffusion method was used to assess the synthesized compounds for antifungal activity against *Aspergillus niger* and *Candida albicans* fungal strains *in vitro* against the standard clotrimazole drug (10 g/disc). Each Petri plate was divided into four quadrants, with I (100 mcg), II (200 mcg) and III (300mcg) discs extracted in three quadrants (discs are soaked overnight in extract solution). Using sterile forceps, one quadrant of standard Clotrimazole 5 mcg was inserted in each quadrant. Petri dishes were set for 1 h of diffusion in the refrigerator at 40 ºC at room temperature [10] followed by incubation for 24 to 48 h at room temperature. The zone of inhibition was measured and then the average of two measurements was recorded.

Molecular docking: *N*-Aryl amides derivatives (**A-H**) with strong experimental antifungal activity point to the need for molecular docking studies to identify a viable target usingAutodock vina 1.5.6 software. ChemDraw Ultra 12.0 was used to draw the structure of synthesized molecules and Gaussian Software 16W was used to optimize the structure [11,12]. The ligand was then generated into PDBQT using the graphical interface programme MGL tools. *endo*-1, 4-Glucanase (PDB id: 1KS5) [10,13-15] and *N*-myristoyltransferase (PDB id: 1NMT) [16-20] from the protein data bank coordinate file were used as antifungal receptor molecules. The grid box was customized using MGL tools in order to execute docking simulations. Autodock Vina was used to find the optimal docked conformation for compounds with proteins as well as their binding affinity. The visual description of the interaction between the ligands and the target protein was deduced using LigPlot+ and PyMol. The 3D coordinates of the target receptor were derived using the 1KS5 and 1NMT -Proteins, and the optimum docked conformation of the tested structures was identified using glide energy, binding energy, active hydrogen bonding sites, and hydrophobic interactions [21].

Toxicity potential prediction: Toxicity risk prediction provides an insight into the potential negative effects of synthesized molecules that could be utilized in drug development and discovery. A pre-computed series of structural fragments was used to assess mutagenic, tumorigenic, irritant and reproductive toxicity [22]. OSIRIS Property Explorer Software was performed to create toxic parameters for the synthesized compound [23].

Bioactivity score assessment: Drug score values show compound's overall potential as a drug candidate. Molinspiration cheminformatic software is a web-based application that predicts the bioactivity of synthesized compounds against common human receptors such G protein-coupled receptors (GPCR) ligands, ion channels, kinases, nuclear receptors, proteases and enzymes [23].

Lipinski's Rule of five: Lipinski's rule of five is useful for characterizing the molecular features of drug molecules that are needed to assess critical pharmacokinetic parameters like absorption, distribution, metabolism, excretion and toxicity (ADMET). The rule is useful in therapeutic development and design. *in silico*, ADMET analysis can predict several significant traits and it is useful for evaluating a molecule's desirable attributes. The current study evaluates ADMET properties such as aqueous solubility (log S), skin permeability (log K_p), lipophilicity, percentage absorption, pharmacokinetics and drug-likeness properties of small molecules using an online portal called SwissADME [24,25].

Computational methods: For the investigated compounds, full geometry optimizations were performed utilizing the DFT at the B3LYP level using Gaussian 16w software. The 6-31G basis set level was used to compute the properties and HOMO-LUMO energies of the investigated compounds. At the same level of approach, Mulliken charge distributions, molecular electro static potential, natural bond analyses and quantum chemical parameters were computed [10]. Gaussian programme output files were viewed using Gaussian view 6.1.

RESULTS AND DISCUSSION

Antifungal activity: The disc diffusion method was used to evaluate the *in vitro* antifungal activity of the synthesized *N*-aryl amides derivatives (**A-H**) against *Aspergillus niger* and *Candida albicans* and compared with clotrimazole (10 g/disc) as a reference. According to study, *N*-aryl amides derivatives (**A-H**) had antifungal activity agai*nst A. niger* and *C. albicans* in zones ranging from 17-23 mm for *A. niger* and 15-30 mm for *C. albicans* (Fig. 1).

The inhibitory results at three different concentrations, 50 g, 100 g and 150 g demonstrated that *N*-aryl amides derivatives are susceptible to fungus at higher concentrations, but not so much at lower concentrations. The growth percentage in comparison to the control was calculated using the formula below, where the control's growth percentage was 100%.

$$\text{Growth (\%)} = \frac{\text{Growth of fungi with compound}}{\text{Growth of fungi with control}} \times 100$$

The antifungal analysis was also assessed in terms of growth percentage compared to the control, where the control's growth is 100%, using the formula below, which reveals the compound's ability to exhibit potency against any fungal stain [10].

$$\text{Inhibition (\%)} = \text{Control}_{\text{Growth percentage}} - \text{Compound}_{\text{Growth percentage}}$$

Compounds **C**, **E** and **H** improved the sensitivity against *A. niger* and *C. albicans*, as indicated in Table-1, with compounds **C** and **H** displaying the most action since both the molecules have chlorine atom [10], whereas the enhanced activity of compound **E** is due the presence of more reactive naphthalene ring. In both fungal strains, compounds **A** and **D** had the least level of activity. Inhibition of fungal growth by the reported compounds, indicate the compounds' broad-spectrum antifungal potentials, which make the synthesized compounds for bioprospecting for antibiotic drugs.

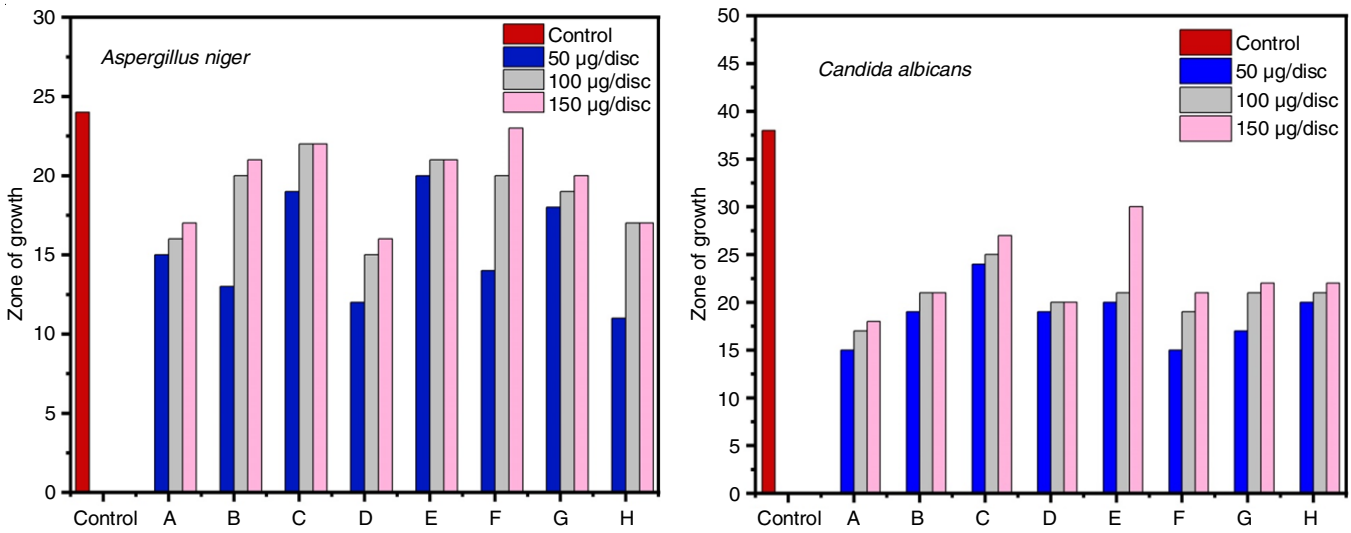

Fig. 1. Zone of growth plot of synthesized compounds (**A-H**) against *Aspergillus niger* and *Candida albicans* tested by disc diffusion assay

TABLE-1
DATA OF PERCENTAGE GROWTH AND INHIBITION AGAINST *Aspergillus niger* AND *Candida albicans*

Compd.	*Aspergillus niger*						*Candida albicans*					
	50 µg/disc		100 µg/disc		150 µg/disc		50 µg/disc		100 µg/disc		150 µg/disc	
	Growth (%)	Inh. (%)	Growth (%)	Inh. (%)	Growth (%)	Inh. (%)	Growth (%)	Inh. (%)	Growth (%)	Inh. (%)	Growth (%)	Inh. (%)
Control	100%	0%	100%	0%	100%	0%	100%	0%	100%	0%	100%	0%
A	62.50	37.50	66.66	33.34	70.83	29.17	39.47	60.53	44.73	55.27	47.36	52.64
B	54.15	45.85	83.33	16.67	87.50	12.50	50.00	50.00	55.26	44.26	55.26	44.26
C	79.16	20.84	91.66	8.34	91.66	8.34	63.15	36.85	65.78	34.22	71.05	28.95
D	50.00	50.00	62.50	37.50	66.66	33.34	50.00	50.00	52.63	47.37	52.63	47.37
E	83.33	16.67	87.50	12.50	87.50	12.50	52.63	47.37	55.26	44.74	78.94	21.06
F	58.33	41.67	83.33	16.67	95.83	4.17	39.47	60.53	50.00	50.00	55.26	44.74
G	75.00	25.00	79.16	20.84	83.33	16.67	44.73	55.27	55.26	44.74	57.89	42.11
H	45.83	54.17	70.83	29.17	70.83	29.17	52.63	47.37	55.26	44.74	57.89	42.11

Molecular docking: The N-myristoyltransferase (1NMT) is essential for viability in a number of human pathogens, including the fungi, *Candida albicans*, which is important in a variety of biological processes with signal transduction pathways, apoptosis [16,18] and significant for the growth of fungal cells [19,20]. *Aspergillus niger* as a mammalian pathogen can secrete large amounts of different cellulases, in which *endo*-1,4-glucanase(1KS5) [15] is the main component which cleave the internal β-1,4-glucosidic bonds to cellooligosaccharides and responsible for the biosynthesis and remodelling the fungi cell wall [26]. As a result, inhibiting these proteins prevents biosynthesis, affecting the cell wall's integrity and consequently leading to the cell death.

Furthermore, the docking interactions between these fugal proteins 1NMT and 1KS5 and the synthesized compounds (A-H) was carried out to identify the most significantly interacting residues and the type of thermodynamic interactions responsible for the binding of these molecules. The docking run produced nine distinct positions for each compound, along with the appropriate binding energy scores; the best-docked poses with the lowest energy from a total of nine poses for each compound were retained. Tables 2 and 3 show the docking findings of the investigated drugs. Fig. 2 illustrate the 2D and 3D depictions of *N*-aryl amides derivatives (**A-H**) interacting with the target receptors 1KS5 and 1NMT, respectively. According to the findings, the investigated compounds interacted extensively with amino acids of the target proteins 1KS5 and 1NMT, with binding energies ranging from -9.7 to -7.5 kcal/mol, which is superior to the binding energy of the conventional drug clotrimazole.

Compound **E** was shown to have the best docking binding energies of -9.6 and -9.7 kcal/mol with the target receptors 1KS5 and 1NMT through three conventional hydrogen bonds [Gln200A-2.89 Å, Asn20A-3.61 Å, Asn63A-3.91 Å and Asp170B-3.01 Å, Pro190A-3.59 Å, Lys194A-3.98 Å], since it contains more reactive naphthalene group attachment. The compounds also had the greatest hydrophobic interactions (six) with the target proteins. This orientation in terms of hydrogen bonding and hydrophobic interactions could help antifungal activity. As a result, *N*-aryl amides derivatives (**A-H**) may be effective at interacting with the target receptor, indicating that the molecules under investigation are biologically active.

Toxicity potential prediction: The toxicity risk predictor looks for fragments in a molecule that could indicate toxicity. The findings clearly revealed that all *N*-aryl amides derivatives (**A-H**), with the exception of compound **E**, are safe and likely

TABLE-2
PREDICTED H-BONDS, H-BOND LENGTH, H-HYDROPHOBIC INTERACTIONS, BINDING ENERGY (kcal/mol) BETWEEN LIGANDS (A-H) AND MACROMOLECULE *Aspergillus niger* (PDB-1KS5)

Compounds	Hydrogen bonds	H-Bond length (Å)	H-bond with	Hydrophobic Interactions	Binding energy (kcal/mol)
A	3	2.80, 3.27, 3.55	Asn63(A), Gln200(A), Asn20(A)	Tyr7(A), Asn20(A), Tyr61(A)	-7.5
B	3	2.79, 3.32, 3.37	Asn63(A), Gln200(A), Asn20(A)	Asn20(A), Tyr61(A), Trp22(A)	-8.0
C	3	3.18, 3.23, 3.98	Asn63(A), Gln200(A), Asn20(A)	Asn20(A), Tyr61(A)	-7.9
D	4	2.91, 3.40, 3.41, 3.80	Gln200(A), Glu204(A), Asn20(A), Asn63(A)	Asn20(A), Trp22(A)	-8.1
E	3	2.89, 3.61, 3.91	Gln200(A), Asn20(A), Asn63(A)	Asn20(A), Tyr61(A), Tyr7(A), Trp22(A)	-9.6
F	3	2.92, 3.53, 3.85	Gln200(A), Asn20(A), Asn63(A)	Asn20(A), Tyr61(A), Tyr7(A), Trp22(A)	-8.7
G	4	2.92, 3.36, 3.48, 3.90	Gln200(A), Glu204(A), Asn20(A), Asn63(A)	Asn20(A), Tyr61(A), Tyr7(A), Trp22(A)	-8.4
H	3	3.23, 3.25, 3.88	Ser111(A), Gln200(A), Asn20(A)	Asn18(A), Tyr7(A), Trp22(A), Phe101(A)	-8.3
Std. (S)	3	2.94, 3.23, 3.67	Asn20(A), Asn63(A), Gln200(A)	Asn20(A), Tyr7(A),	-6.5

TABLE-3
PREDICTED H-BONDS, H-BOND LENGTH, H-HYDROPHOBIC INTERACTIONS, BINDING ENERGY (kcal/mol) BETWEEN LIGANDS (A-H) AND MACROMOLECULE *Candida albicans* (PDB-1NMT)

Compounds	Hydrogen bonds	H-Bond length (Å)	H-bond with	Hydrophobic Interactions	Binding energy (kcal/mol)
A	5	2.80, 3.72, 4.00, 4.06, 4.10	Gln207(B), Asp170(B), Gln207(B), Asp170(B), Trp206(B)	Pro62(B), Leu66(B), Asp170(B), Pro190(A), Val191(A), Ile205(B)	-8.3
B	3	3.19, 3.72, 4.09	Lys284(C), Lys436(B) Ser280(C)	Pro219(B), Tyr283(C), Phe414(B)	-8.6
C	4	2.80, 3.25, 3.54, 3.91	Glu109(B), Gly213(B), Ser214(B), Tyr210(B)	Leu415(B)	-8.4
D	2	3.03, 3.31	Thr197(B), Asn201(B)	Pro217(B), Leu216(B), Thr197(B), Val168(C), Ile193(B), Leu294(C), Phe420(B)	-8.0
E	3	3.01, 3.59, 3.98	Asp170(B), Pro190(A), Lys194(A)	Leu216(A), Val168(B), Ile193(B), Leu294(C), Phe420(B), Ile169(B),	-9.7
F	3	3.09, 3.22, 3.96	Lys284(C), Lys436(B) Ser280(C)	Pro219(B), Phe414(B)	-8.9
G	2	3.09, 3.23	Thr197(B), Asn201(B)	Val168(B), Ile193(B), Leu294(C), Phe420(B), Pro217(B), Thr197(B)	-8.3
H	3	2.99, 3.92, 3.98	Lys436(B), Lys284(C), Ser280(C)	Ile215(B), Phe414(B), Thr222(B), Tyr283(C), Lys284(C)	-8.6
Std. (S)	2	3.33, 3.84	Asp64(B), Val168(C)	Ile63(B), Val168(C), Thr197(B), Phe420(B)	-7.5

to have almost no toxicity in terms of mutagenicity, tumorigenicity, irritant and reproductive system effects. According to Table-4, all of the compounds performed well in screening, with the best drug score values (DS = 0.870.85), with the exception of compound **E**, which had lower values (DS = 0.32).

Bioactivity score assessment: Different characteristics such as binding to G protein-coupled receptor (GPCR) ligand and nuclear receptor ligand, ion channel modulation, kinase inhibition, protease inhibition and enzyme activity inhibition were used to compute the bioactivity scores of the synthesized compounds. All of the parameters were estimated using the online software Molinspiration, which projected that the synthesized compounds would have significant biological activity. The bioactivity score is given in Table-5. It is known that if the bioactivity score for molecules is greater than 0.0, the group is active; if it is between -5.0 and 0.0, the molecule is moderately

TABLE-4
TOXIC POTENTIALITY OF THE SYNTHESIZED COMPOUNDS (**A-H**)

Compounds	Toxic potentiality (K_i or IC_{50} in nmol/L)				
	Mutagenic	Tumorigenic	Reproductive	Irritant	Drug score None < 0.8 < High
A	None	None	None	None	0.867
B	None	None	None	None	0.861
C	None	None	None	None	0.874
D	None	None	None	None	0.875
E	Medium	High	None	None	0.326
F	None	None	None	None	0.861
G	None	None	None	None	0.873
H	None	None	None	None	0.857

	2D representation of the compounds (A-H) with *Aspergillus niger* (PDB-1 KS5)	3D representation of the compounds (A-H) with *Aspergillus niger* (PDB- 1KS5)	2D representation of the compounds (A-H) with *Candida albicans* (PDB-1NMT)	3D representation of the compounds (A-H) with *Candida albicans* (PDB-1NMT)
A	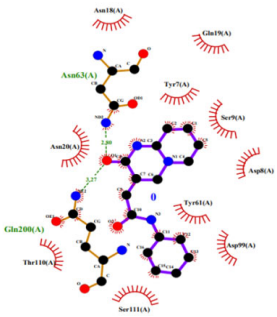	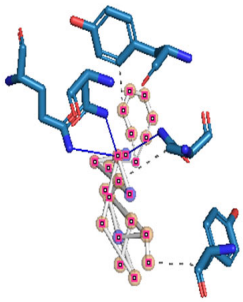	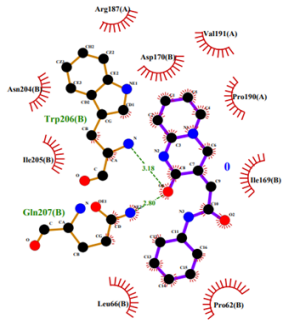	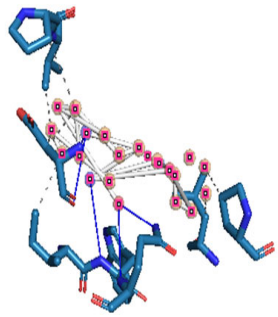
B	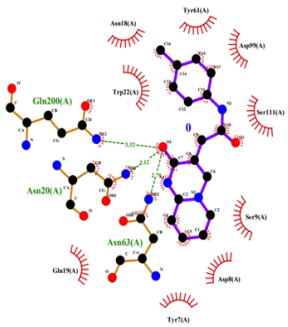	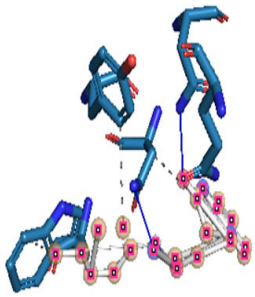	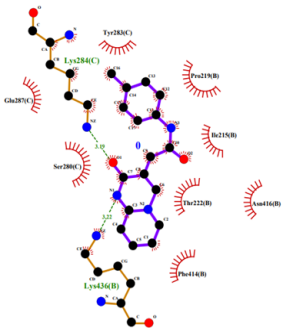	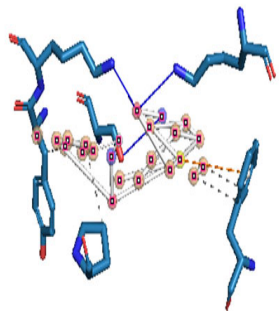
C	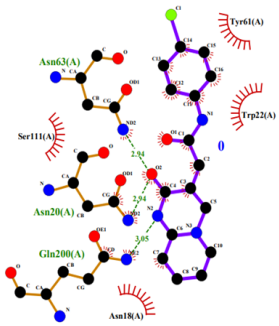	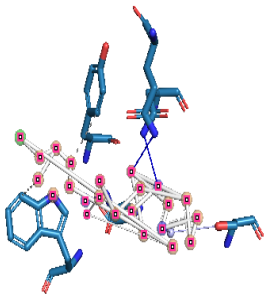	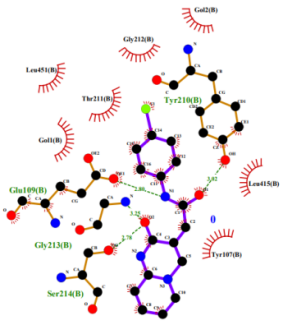	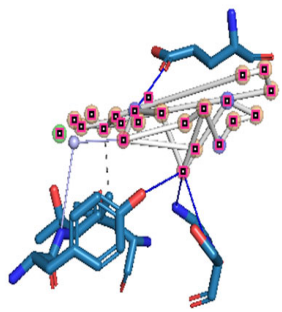
D	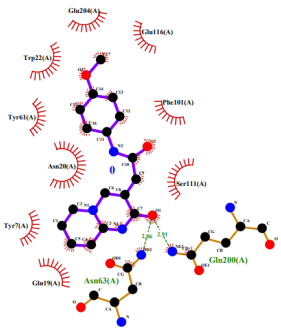	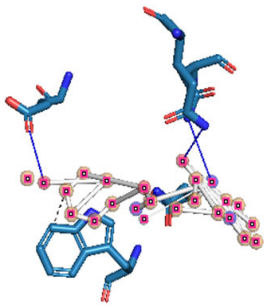	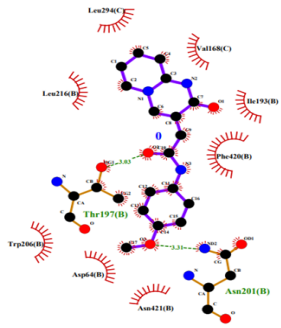	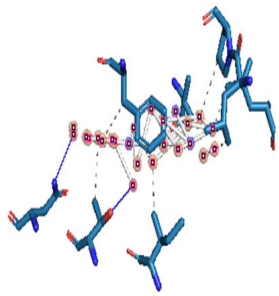
E	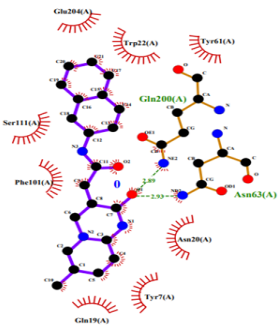	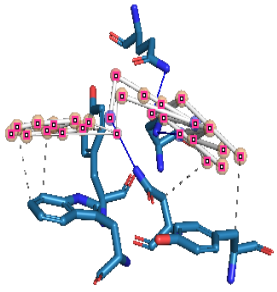	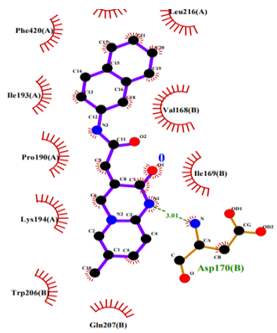	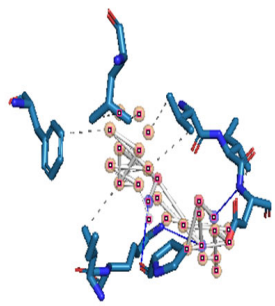

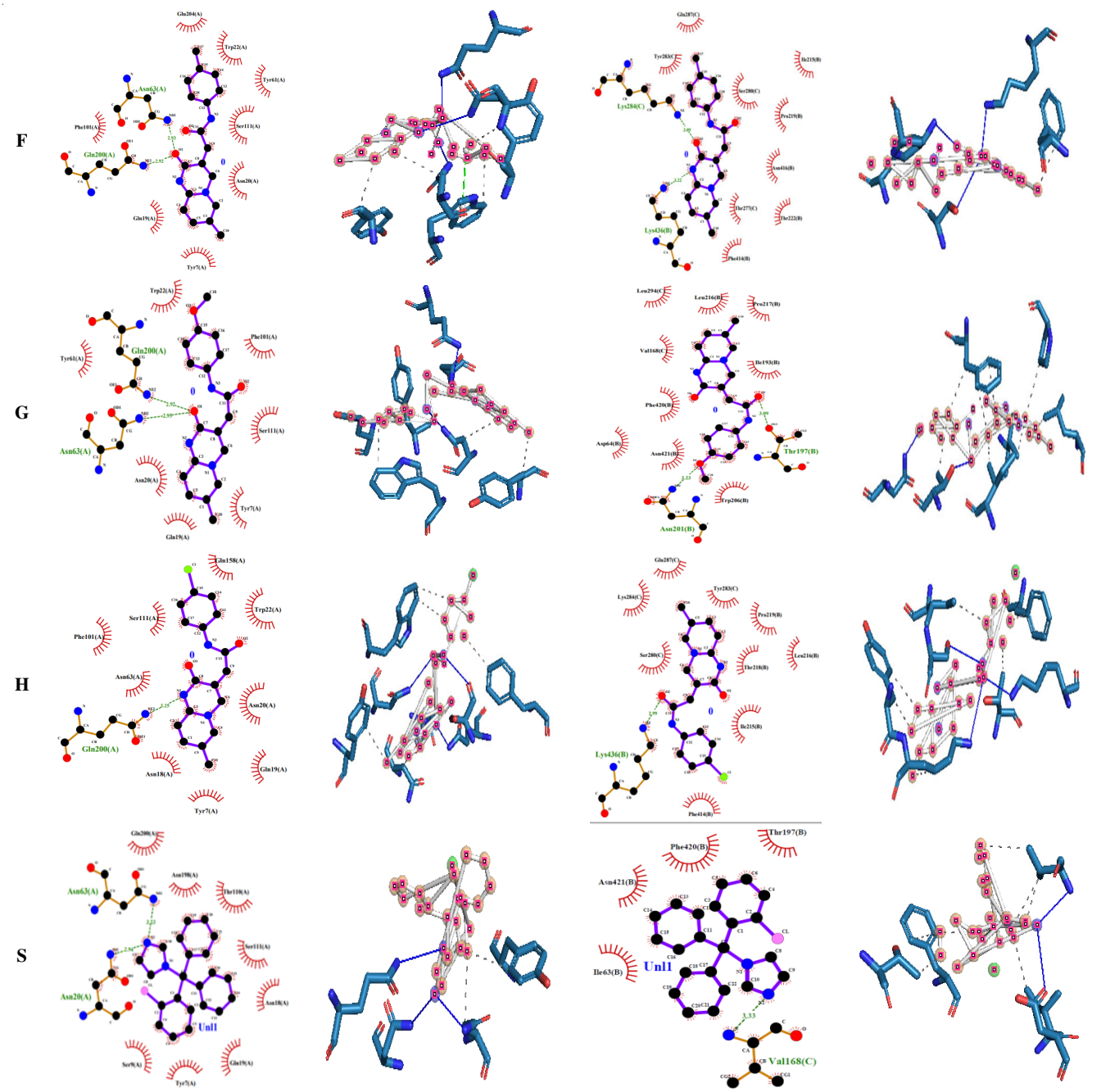

Fig. 2. 2D and 3D representation of the interaction of the compounds (**A-H**) with macromolecule *Aspergillus niger* (PDB-1KS5) and *Candida albicans* (PDB-1NMT)

TABLE-5
BIOACTIVITY SCORE OF THE SYNTHESIZED COMPOUNDS (**A-H**)

Compounds	Parameters of bioactivity score					
	GPCR ligand	Ion channel modulator	Kinase inhibitor	Nuclear receptor ligand	Protease inhibitor	Enzyme inhibitor
A	-0.49	-0.59	-0.58	-0.77	-0.71	-0.42
B	-0.49	-0.66	-0.58	-0.74	-0.71	-0.48
C	-0.45	-0.57	-0.55	-0.74	-0.69	-0.45
D	-0.46	-0.63	-0.54	-0.68	-0.65	-0.44
E	-0.34	-0.54	-0.44	-0.62	-0.56	-0.35
F	-0.47	-0.67	-0.59	-0.77	-0.73	-0.47
G	-0.47	-0.67	-0.58	-0.73	-0.72	-0.48
H	-0.45	-0.65	-0.59	-0.77	-0.76	-0.48

active; and if it is less than -5.0, the product is inert [23]. The bioactivity scores of *N*-aryl amides derivatives (**A-H**) ranged from -5.0 to 0.0, among the entire, compound **E** exhibits higher values (-0.46, -0.63, -0.54, -0.68, -0.65 -0.44) which intimates that compound **E** is more active molecule then the others, and can behave as potential drugs with minor chemical modifications.

Lipinski's rule of five: The absorption, distribution, metabolism and excretion (ADME) of a drug in the human body provides the information about the oral absorption or membrane permeability of the evaluated molecule using various rules such as Lipinski's rule of five, which states that compounds with good membrane permeability should have MW ≤ 500, RB ≤ 10, ClogP ≤ 5 , HBA ≤ 10 and HBD ≤ 5 [27]. All of the compounds satisfied Lipinski's rule and the values of molecular properties are tabulated in Table-6. The value of molar refractivity of the studied compounds lies within its range *i.e*. 40-130 similarly the value of TPSA of all the studied compound lies in the range 63.46-72.69 Å^2, which is under the 140 Å^2 upper limit of TPSA [28]. All the compounds show high GI absorption, whereas compounds **D** and **G** are not available for BBB permeant. Any drug molecules satisfying the 'rule of five' with a bioavailability (BA) score of 0.55 are considered as sufficiently absorbable *via* oral route [29]. The bioavailability's of all the compounds are same which is 0.55. It means that all the compounds have good binding affinity and theoretically would not have any problem with oral bioavailability.

Frontier molecular orbitals (FMOs): The B3LYP/6-31G methodology was used to optimize the structures of all the compounds. Fig. 3 depicts the HOMO-LUMO energy gap of the compounds (**A-H**). Compounds **D** and **G** have a slightly lower HOMO-LUMO energy gap than the other six compounds (Table-7), which could be due to the –OEt group's electron donating tendency [21]. As a result, compounds D and G are softer than any other compounds. The hardness of an atom dictates how well it resists charge transfer to another atom or metal surface. Compounds **D** and **G** were found to have lower hardness and higher softness values than the other compounds studied. As a result, compounds **D** and **G** are found to be more reactive. Electronegativity is a chemical property that defines a molecule's proclivity to attract electrons. In present case, compound C has a high electronegative value, making it the best electron acceptor among all compounds. It could be due to the presence of chlorine atom.

Molecular electrostatic potential (MEP): Based on the electrostatic potential distribution, different shades reflect the different values of electrostatic potential at the surface; red - most electronegative electrostatic potential, blue-most positive electrostatic potential and green-zero potential [22,30]. For all *N*-aryl amides derivatives (**A-H**), it is found that the more negative electrostatic potential is around the carbonyl oxygen, yellow colour in C-N represents medium negative electrostatic potential, whereas more positive electrostatic potential is found around the pyridopyrimidine ring at the first position. Hydrogen atoms connected to heterocyclic rings have zero potential (Fig. 4).

Mulliken charge analysis: Fig. 5 depicts the Mulliken charge values for the constituent atoms of the examined molecules. The hydrogen and chlorine atoms in the molecule are positively charged and referred to as donors, whereas carbon and other atoms are negatively charged and referred to as acceptors. The hydrogen atom nearest the oxygen atom has the most positive charge [30]. This is because oxygen atoms are electro-

TABLE-6
ADME PARAMETERS OF SYNTHESIZED COMPOUNDS (**A-H**)

Compd.	MW g/mol ≤ 500	RB ≤ 10	NHA ≤ 10	NHB ≤ 5	MR	TPSA (Å^2)	C log P ≤ 5	log S	GI absorption	BBB	P-gp	CYP1A2 inhibitor	log k$_p$ (cm/s)	Drug lineness (Lipinski violation)	Bioavailability score
A	297.29	3	3	1	81.51	63.46	1.42	Soluble	High	Yes	No	Yes	-7.36	Yes	0.55
B	293.32	3	3	1	86.47	63.46	1.78	Soluble	High	Yes	No	Yes	-7.19	Yes	0.55
C	313.74	3	3	1	86.52	63.46	2.03	Soluble	High	Yes	No	Yes	-7.13	Yes	0.55
D	309.32	4	4	1	88.00	72.69	1.43	Soluble	High	No	No	No	-7.51	Yes	0.55
E	343.38	3	3	1	103.9	63.46	2.58	Soluble	High	Yes	No	Yes	-6.92	Yes	0.55
F	307.35	3	3	1	91.44	63.46	2.01	Soluble	High	Yes	No	Yes	-7.34	Yes	0.55
G	323.35	4	4	1	92.96	72.69	1.67	Soluble	High	No	No	No	-7.71	Yes	0.55
H	327.76	3	3	1	91.48	63.46	2.18	Soluble	High	Yes	No	Yes	-7.27	Yes	0.55

TABLE-7
GLOBAL REACTIVE PARAMETERS CALCULATED FOR COMPOUNDS (**A-H**)

Parameters	**A**	**B**	**C**	**D**	**E**	**F**	**G**	**H**
E_{HOMO} (eV)	-0.20350	-0.19704	-0.21166	-0.18714	-0.19063	-0.19565	-0.18569	-0.21023
E_{LUMO} (eV)	-0.09179	-0.09064	-0.09728	-0.09013	-0.09057	-0.08840	-0.08810	-0.09497
Energy gap (Δ) (eV)	0.11171	0.1064	0.11438	0.09701	0.10006	0.10725	0.09759	0.11526
Ionization energy (I) (eV)	0.20350	0.19704	0.21166	0.18714	0.19063	0.19565	0.18569	0.21023
Electron affinity (A) (eV)	0.09179	0.09064	0.09728	0.09013	0.09057	0.08840	0.08810	0.09497
Electronegativity (χ)	0.147645	0.14384	0.15447	0.138635	0.1406	0.142025	0.13689	0.1526
Chemical potential (μ) (eV)	-0.147645	-0.14384	-0.15447	-0.138635	-0.1406	-0.142025	-0.13689	-0.1526
Global hardness (η) (10^1eV)	0.55855	0.532	0.5719	0.48505	0.5003	0.53625	0.48795	0.5763
Global softness (S) (eV^{-1})	1.7903	1.87970	1.74855	2.06164	1.99880	1.86480	2.04930	1.73520
Electrophilicity index (ω) (eV)	0.19514	0.19445	0.20861	0.19812	0.19757	0.18808	0.19200	0.20204
Dipole moment (Debye)	9.6374378	9.1350752	12.72428	9.0303144	10.710887	9.8954162	9.955893	13.509229

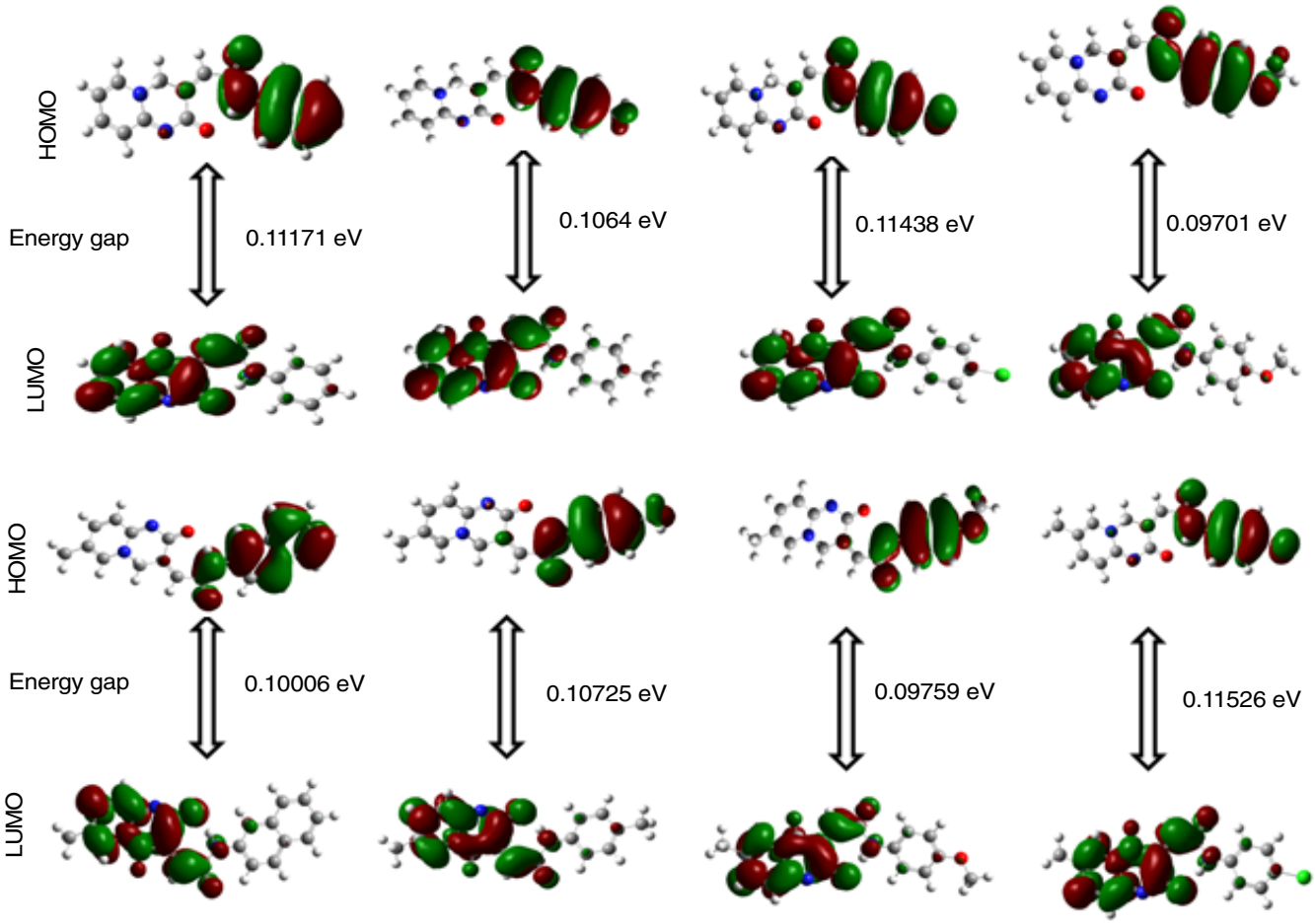

Fig. 3. HOMO and LUMO structure of the compounds (**A-H**) generated from B3LYP method using 6-31G basis set

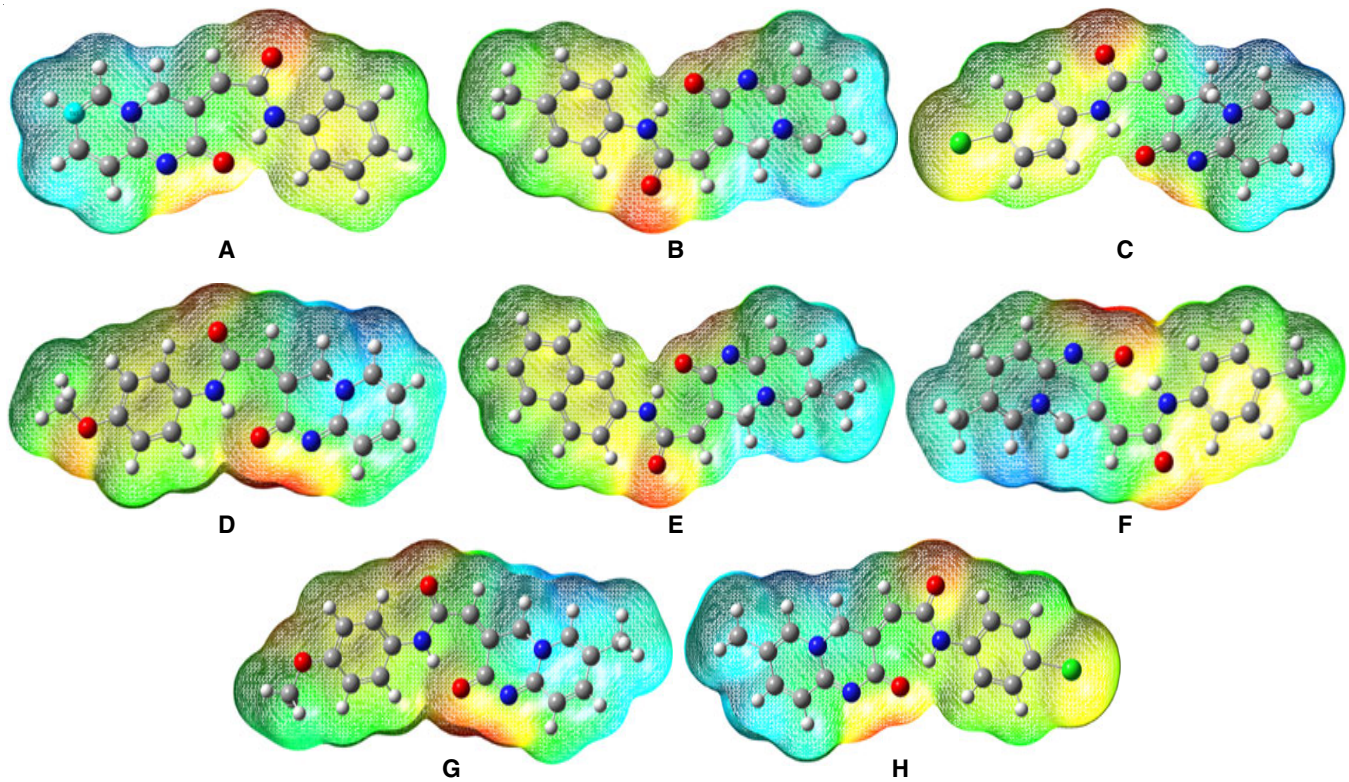

Fig. 4. Molecular electrostatic potential (MEP) of compounds (**A-H**)

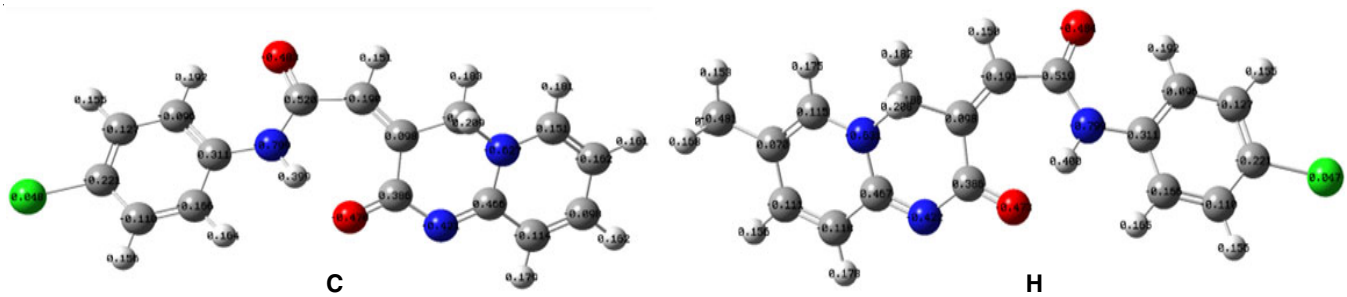

Fig. 5. Mulliken charge values for compounds **C** and **H** with positively charged chlorine atom

negative. The distribution of partial charges on the skeleton atoms indicates that electrostatic repulsion or attraction between atoms can contribute significantly to the intermolecular and intramolecular interaction estimated using the DFT/B3LYP approach.

Conclusion

The antifungal activity of *N*-aryl amides of pyrido[1,2-*a*]-pyrimidin-2-one derivatives (**A-H**) against two fungi (*Aspergillus niger* and *Candida albicans*) were investigated. Compounds **E** and **C** have strong antifungal action against *A. niger* and *C. albicans*, while other compounds exhibited significant anti-fungal activity. Computational analysis and molecular docking with probable receptors or prediction of bioactivity score and physico-chemical attributes can be used to predict the total activity spectrum of biologically active substances. Compound E showed the highest docking binding energy against target receptors 1KS5 and 1NMT in docking findings, indicating a solid agreement between docking studies and antifungal activity results. Moreover, the MEP, Mulliken charge distribution and Fukui functions were also calculated in order to identify the nucleophilic and electrophilic approaches. Furthermore, the HOMO-LUMO energy gap for compounds **D** and **G** were slightly lower in comparison to the other six compounds, which could be due to the electron donating tendency of –OEt group present. Pharmacophore calculations, such as ADME, BBB, and toxicity, were also performed and all the *N*-aryl amides of pyrido[1,2-*a*]-pyrimidin-2-one derivatives demonstrated drug-like characteristics. According to the AMDET study, all *N*-aryl amides of pyrido[1,2-*a*]-pyrimidin-2-one derivatives (**A-H**) are non-carcinogenic, low toxic and water soluble. The drug-likeness investigation demonstrated that the tested compounds (**A-H**) show promising results, indicating that the examined molecules can be employed as an intermediate in numerous drug synthesis.

CONFLICT OF INTEREST

The authors declare that there is no conflict of interests regarding the publication of this article.

REFERENCES

1. M. Ivanov, A. Ciric and D. Stojkovic, *Int. J. Mol. Sci.*, **23**, 2756 (2022); https://doi.org/10.3390/ijms23052756
2. F. Buron, J.Y. Mérour, M. Akssira, G. Guillaumet and S. Routier, Eur. J. Med. Chem., 95, 76 (2015); https://doi.org/10.1016/j.ejmech.2015.03.029
3. T. Sasada, F. Kobayashi, N. Sakai and T. Konakahara, *Org. Lett.*, **11**, 2161 (2009); https://doi.org/10.1021/ol900382j
4. R. Qingyun, T. Xiaosong and H. Hongwu, *Curr. Org. Synth.*, **8**, 752 (2011); https://doi.org/10.2174/157017911796957366
5. K.N. Kumar, K. Sreeramamurthy, S. Palle, K. Mukkanti and P. Das, *Tetrahedron Lett.*, **51**, 899 (2010); https://doi.org/10.1016/j.tetlet.2009.11.127
6. O. Nagaraja, Y.D. Bodke, I. Pushpavathi and S. Ravi Kumar, *Heliyon*, **6**, e04245 (2020); https://doi.org/10.1016/j.heliyon.2020.e04245
7. M. Huo, L. Zhao, T. Wang, W. Zong and R. Liu, *J. Mol. Recognit.*, **33**, e2822 (2020); https://doi.org/10.1002/jmr.2822
8. E. Yuriev, M. Agostino and P.A. Ramsland, *J. Mol. Recognit.*, **24**, 149 (2011); https://doi.org/10.1002/jmr.1077
9. S. Venugopal, A. Anbazhagan, M. Rajeswari and S. Sundaram, *J. Indian Chem. Soc*., **97**, 1584 (2020).
10. A. Kumer and M.W. Khan, *J. Mol. Struct.*, **1245**, 131087 (2021); https://doi.org/10.1016/j.molstruc.2021.131087
11. O. Trott and A.J. Olson, *J. Comput. Chem.*, **31**, 455 (2010); https://doi.org/10.1002/jcc.21334
12. S. Forli, R. Huey, M.E. Pique, M.F. Sanner, D.S. Goodsell and A.J. Olson, *Nat. Protoc.*, **11**, 905 (2016); https://doi.org/10.1038/nprot.2016.051
13. S.A. Gandhi, R.D. Modh, U.H. Patel, B.D. Patel, K.H. Chikhalia and A.C. Patel, *Mol. Cryst. Liq. Cryst.*, **708**, 98 (2020); https://doi.org/10.1080/15421406.2020.1811023
14. S. Dacrory, A.H. Hashem and M. Hasanin, *Environ. Nanotechnol. Monit. Manag.*, **15**, 100453 (2021); https://doi.org/10.1016/j.enmm.2021.100453
15. S. Khademi, D. Zhang, S.M. Swanson, A. Wartenberg, K. Witte and E.F. Meyer, *Acta Crystallogr. D Biol. Crystallogr.*, **58**, 660 (2002); https://doi.org/10.1107/S0907444902003360
16. S.S. Meenambiga and K. Rajagopal, *J. Appl. Pharm. Sci.*, **8**, 37 (2018); https://doi.org/10.7324/JAPS.2018.8707
17. M.L. Beatrice, S.M. Delphine, M. Amalanathan and H.M. Robert, *Asian J. Chem.*, **32**, 2475 (2020); https://doi.org/10.14233/ajchem.2020.22718
18. F. Qi, Q. Qi, J. Song and J. Huang, *Chem. Biodivers.*, **18**, e2000804 (2021); https://doi.org/10.1002/cbdv.202000804
19. F. Qi, S. Wang, C. Wei, Z. Guo, J. Song and J. Huang, *Rev. Roum. Chim.*, **66**, 509 (2021); https://doi.org/10.33224/rrch.2021.66.6.03
20. F. Qi, J. Song and J. Huang, *J. Mol. Struct.*, **1224**, 129044 (2021); https://doi.org/10.1016/j.molstruc.2020.129044
21. M. B, Y.D. Bodke, N. O, L.T. N, N. G and S. Ma, *J. Mol. Struct.*, **1246**, 131170 (2021); https://doi.org/10.1016/j.molstruc.2021.131170
22. M.I. Azad, T. Khan, A.K. Maurya, M. Irfan Azad, N. Mishra and A.M. Alanazi, *J. Mol. Recognit.*, **34**, e2918 (2021); https://doi.org/10.1002/jmr.2918
23. T. Khan, S. Dixit, R. Ahmad, S. Raza, I. Azad, S. Joshi and A.R. Khan, *J. Chem. Biol.*, **10**, 91 (2017); https://doi.org/10.1007/s12154-017-0167-y

24. R. Dumpati, V. Ramatenki, R. Vadija, S. Vellanki and U. Vuruputuri, *J. Mol. Recognit.*, **31**, e2706 (2018); https://doi.org/10.1002/jmr.2706
25. H.S.N. Prasad, A.P. Ananda, T.N. Lohith, P. Prabhuprasad, H.S. Jayanth, N.B. Krishnamurthy, M.A. Sridhar, L. Mallesha and P. Mallu, *J. Mol. Struct.*, **1247**, 131333 (2022); https://doi.org/10.1016/j.molstruc.2021.131333
26. C.H. Li, H.R. Wang and T.R. Yan, *Molecules*, **17**, 9774 (2012); https://doi.org/10.3390/molecules17089774
27. A. Fatima, G. Khanum, S. Savita, K. Pooja, I. Verma, N. Siddiqui and S. Javed, *J. Mol. Liq.*, **346**, 117150 (2022); https://doi.org/10.1016/j.molliq.2021.117150
28. N. Agarwal, I. Verma, N. Siddiqui and S. Javed, *J. Mol. Struct.*, **1245**, 131046 (2021); https://doi.org/10.1016/j.molstruc.2021.131046
29. Y.C. Martin, *J. Med. Chem.*, **48**, 3164 (2005); https://doi.org/10.1021/jm0492002
30. A.M. Deghady, R.K. Hussein, A.G. Alhamzani and A. Mera, *Molecules*, **26**, 3631 (2021); https://doi.org/10.3390/molecules26123631

J. Indian Chem. Soc.,
Vol. 97, No. 9b, September 2020, pp. 1584-1589

Synthesis, characterization and molecular docking of N-aryl amides of pyrido[1,2-*a*]pyrimidin-2-ones as potential antibacterial agents

Sharulatha Venugopal, Abinaya Anbazhagan*, M. Rajeswari and Sivakamasundari Sundaram

Department of Chemistry, Avinashilingam Institute for Home Science and Higher Education for Women, Coimbatore-641 043, Tamil Nadu, India

E-mail: abinayachemist@gmail.com

Manuscript received online 26 July 2020, accepted 30 August 2020

Nitrogen-containing heterocyclic compounds play the most key role in the discovery of new drugs. Among all, pyrimidine possesses a wide spectrum because of its positive pharmacological and biological properties. Some novel amides of pyrido[1,2-*a*]pyrimidine-2-one acetic acids were synthesized, and the structure of the products was confirmed by FTIR, Mass, ^{1}H NMR, and ^{13}C NMR spectral analysis. The compounds synthesized were evaluated for their *in vitro* antibacterial activity against *Bacillus subtilis* and *Escherichia coli* by the disc diffusion method. All the compounds showed moderate antibacterial activity. Out of the all synthesized compounds(*Z*)-*N*-(naphthalene-2-yl)-2-(2-oxo-7-methyl-2*H*-pyrido[1,2-*a*]pyrimidin-3(4*H*)-ylidene)acetamide and (2-oxo-2*H*-pyrido[1,2-*a*]pyrimidin-3(4*H*)-ylidene)-*N*-phenylacetamide showed high sensitivity to the bacteria *Bacillus subtilis.* While in case of *Escherichia coli* compound *N*-(4-methoxyphenyl)-2-(2-oxo-2*H*-pyrido[1,2-*a*]pyrimidin-3(4*H*)-ylidene)acetamide showed higher activity. Further the newly synthesized compounds docking studies were performed against the active site of 1T9U and 3UZ0 protein.

The compound (*Z*)-*N*-(naphthalene-2-yl)-2-(2-oxo-7-methyl-2*H*-pyrido[1,2-*a*]pyrimidin-3(4*H*)ylidene)acetamide possess great binding affinity towards 3UZ0 and 1T9U bacterial protein targets and possess bioavailability. Based on the docking result, we claim that (*Z*)-*N*-(naphthalene-2-yl)-2-(2-oxo-7-methyl-2*H*-pyrido[1,2-*a*]pyrimidin-3(4*H*)-ylidene)acetamide could serve as an effective antimicrobial compound to treat bacterial infections.

Keywords: Pyridopyrimidine, amides, pyrido[1,2-*a*]pyrimidine-2-one acetic acids, antibacterial activity, molecular docking, 3UZ0 and 1T9U protein.

Introduction

The heterocyclic compounds are the important scaffolds in the discovery of new drugs. The study of these compounds is of great significance in both theoretical and practical aspects[1]. Medicinal chemists are interested in nitrogen-containing heterocyclic compounds, because they are the fundamental building blocks for the development of novel compounds with biological properties. Organic compounds with nitrogen show better biological activity than non-nitrogen compounds. One such *N*-heterocyclic compounds exhibiting significant pharmacological activities is pyrimidines. Pyrimidines are essential constituent present in all living matter[2]. A broad spectrum of biological activities possessed by pyrimidine like including antibacterial, antifungal, antiviral, antitubercular, anti-inflammatory, anticancer, antimalarial, anti-HIV activity[3].

Serious challenges to physicians towards drug-resistant bacterial strains pose because they cause numerous recurrent infections in humans. *Pseudomonas aeruginosa* (*P. aeruginosa*), *Escherichia coli* (*E. coli*), *Streptococcus pyogenes* (*S. pyogenes*) such bacterial strains gained attention because of their ability to cause Cystic fibrosis, chronic lung infection in humans. Therefore, a novel compound has to be identified to avoid the detrimental effects on drug-resistant bacterial strains. This article describes the use of N-aryl amides of pyrido[1,2-*a*]pyrimidin-2-ones as a potential antimicrobial agent targeting *Escherichia coli* (*E. coli*) and *Bacillus subtilis* (*B. subtilis*) subcellular proteins[4].

The experimental binding modes and affinities of small molecules within the particular receptor target binding site can be predicted using docking methodology. Presently it is used as a standard computational tool in drug design for

ineffective screening studies and direct compound optimization to find new biologically active molecules[5]. Autodock is a suite of free, open-source software and it has been extensively used in drug discovery[6]. Compared with the molecular docking software Autodock vina has approximately two orders of magnitude speed-up in comparison with other docking softwares[7].

In this article, we confirm the antibacterial nature of synthesized *N*-aryl amides of pyrido[1,2-*a*]pyrimidin-2-ones by molecular docking studies. These study findings indicate bioavailability and supportive molecular interaction with amino acids present on selected bacterial subcellular proteins active site[4].

Materials and methods

Melting points were recorded using Biochem melting point and are uncorrected. The infrared (IR) spectrum was recorded in the KBr pellet technique using Perkin-Elmer spectrophotometer**.** Absorption frequencies were quoted in reciprocal centimeters. Nuclear Magnetic Resonance (^{1}H NMR and ^{13}C NMR) spectrum were determined by Bruker modern 400 MHz NMR instrument in $CDCl_3$ solvent, with tetramethylsilane as the internal reference. Chemical shifts were quoted in parts per million (ppm). Mass experiments were performed on GC (T 8000 TOP CE) and combined with a mass spectrometer (Md 800 FIS ONS). Reagent grade solvents and reagents used for the synthesis and standard methods were carried out for purification. Chromatographic columns packed with silica gel were used for purification of the crude products.

General procedure:

A blend of 2-oxo-2*H*-pyrido[1,2-*a*]pyrimidin-3(4*H*)-ylidene acetic acid (0.1 mole) and purified thionyl chloride (0.20 mole) was stirred at room temperature under exclusion of moisture till the solution was complete. The thionyl chloride excess was distilled off under reduced pressure. The residue was recovered by using anhydrous ether (25 ml) and gradually added to a well cooled and stirred mixture of aniline (0.02 mole) in dry ether (25 ml). After the addition, it was set aside for a few minutes and ice water poured into it. The precipitated solid was filtered, dried, and purified by column chromatography.

Physical properties and spectral data:

*2-Oxo-2H-pyrido[1,2-a]pyrimidin-3(4H)-ylidene)-N-phenylacetamide (**A**):*

2-Oxo-2*H*-pyrido[1,2-*a*]pyrimidin-3(4*H*)-ylidene acetic acid: 2.04 g; thionyl chloride: 7 ml; aniline: 2.5 g; ether: 50 ml; yield 3 g (66%); m.p. 228–230°C; IR $(\gamma)_{max}$, cm^{-1}: 3010 (-NH), 1722 (-CO), 1690 (-CO); ^{1}H NMR (400 MHz, $CDCl_3$, γ, ppm): 4.5 (2H, s, $-CH_2$), 6.3 (1H, d, -CH), aromatic and pyridine ring 7–8 (8H, m, =CH), 9.1 (1H, s(b), -NH); ^{13}C NMR (300 MHz, $CDCl_3$, δ, ppm): 174.9 (C=O), 168.5 (amide C=O), ArC (115.2, 119.2, 122.4, 126.6, 126.7, 127.6, 128.4, 128.47, 128.6, 129.2, 132.7, 134.8), 141.1 (CH), 95.3 (CH_2); GC-MS: *m/z* 280 (M+1).

*(Z)-2-(2-Oxo-2H-pyrido[1,2-a]pyrimidin-3(4H)-ylidene)-N-(p-tolyl)acetamide (**B**):*

2-Oxo-2*H*-pyrido[1,2-*a*]pyrimidin-3(4*H*)-ylidene acetic acid: 2.04 g; thionyl chloride: 7 ml; *p*-toludine: 2.7 g; ether: 50 ml; yield 2.8 g (59%); m.p. 249–251°C; IR $(\gamma)_{max}$, cm^{-1}: 3016 (-NH), 1728 (-CO), 1688 (-CO); ^{1}H NMR (400 MHz, $CDCl_3$, δ, ppm): 4.5 (2H, s, $-CH_2$), 6.8 (1H, d, -CH), aromatic and pyridine ring 7–8 (8H, m, =CH), 9.1 (1H, s(b), -NH), 2.0 (3H, s, $-CH_3$); ^{13}C NMR (300 MHz, $CDCl_3$, δ, ppm): 169.2 (C=O), 166.0 (amide C=O), ArC (103.8, 121.5, 122.4, 129.2, 134.6, 135.7, 136.8, 147.2, 157.6, 161.6), 141 (CH), 49.6 (CH_2), 21.3 (CH_3); GC-MS: *m/z* 292 (M+1).

*N-(4-Methoxyphenyl)-2-(2-oxo-2H-pyrido[1,2-a]pyrimidin-3(4H)ylidene)acetamide (**C**):*

2-Oxo-2*H*-pyrido[1,2-*a*]pyrimidin-3(4*H*)-ylidene acetic acid: 2.04 g; thionyl chloride: 7 ml; *p*-anisidine: 3.1 g; ether: 50 ml; yield 3.1 g (62%); m.p. 245–246°C; IR $(\gamma)_{max}$, cm^{-1}: 3018 (-NH), 1730 (-CO), 1691 (-CO); ^{1}H NMR (400 MHz, $CDCl_3$, γ, ppm): 4.2 (2H, s, $-4CH_2$), 6.5 (1H, d, -CH), aromatic and pyridine ring 7–8 (8H, m, =CH), 9.2 (1H, s(b), -NH), 3.8 (3H, s, $-OCH_3$); ^{13}C NMR (300 MHz, $CDCl_3$, δ, ppm): 171.2 (C=O), 167.4 (amide C=O), ArC (103.9, 134.6, 147.1, 121.5, 162.4, 157.2, 122.6, 129.9, 114.5, 158.9), 139.4 (CH), 47.3 (CH_2), 55.8 (CH_3); GC-MS: *m/z* 308 (M+1).

*N-(4-Chlorophenyl)-2-(2-oxo-2H-pyrido[1,2-a]pyrimidin-3(4H)ylidene)acetamide (**D**):*

2-Oxo-2*H*-pyrido[1,2-*a*]pyrimidin-3(4*H*)-ylidene acetic

acid: 2.04 g; thionyl chloride: 7 ml; *p*-chloroaniline: 3.2 g; ether: 50 ml; yield 3.5 g (67%); m.p. 257–258°C; IR $(\gamma)_{max}$, cm^{-1}: 3110 (-NH), 1758 (-CO), 1672 (-CO); ^1H NMR (400 MHz, $CDCl_3$, δ, ppm): 4.6 (2H, s, $-CH_2$), 6.8 (1H, d, -CH), aromatic and pyridine ring 7–8 (8H, m, =CH), 9.0 (1H, s(b), -NH); ^{13}C NMR (300 MHz, $CDCl_3$, δ, ppm): 171.8 (C=O), 165.2 (amide C=O), ArC (104.3, 134.5, 146.01, 159.1, 120.9, 156.2, 135.7,121.7, 129, 133.3), 139.4 (CH), 53.2 (CH_2); GC-MS: *m/z* 313 (M+1).

*(Z)-N-(Naphthalene-2-yl)-2-(2-oxo-7-methyl-2H-pyrido [1,2-a]pyrimidin-3(4H)-ylidene)acetamide (**E**):*

2-Oxo-7-methyl-2*H*-pyrido[1,2-*a*]pyrimidin-3 (4*H*)-ylidene acetic acid: 2.18 g; thionyl chloride: 7 ml; naphthylamine 2.6 g; ether: 50 ml; yield 3 g (62%); m.p. 274–275°C; IR $(\gamma)_{max}$, cm^{-1}: 3110 (-NH), 1742 (-CO), 1678 (-CO); ^1H NMR (400 MHz, $CDCl_3$, δ, ppm): 4.3 (2H, s, $-CH_2$), 6.5 (1H, d, -CH), aromatic and pyridine ring 7–8 (8H, m, =CH), 9.0 (1H, s(b), -NH), 2.12 (3H, s, $-CH_3$); ^{13}C NMR (300 MHz, $CDCl_3$, δ, ppm): 168.9 (C=O), 165.7 (amide C=O), ArC (120.5, 119.6, 142.9, 122.2, 160.7, 157.4, 135.4, 119.9, 116.7, 129, 133.7, 126.8, 126.5, 124.6, 125.3, 121.4), 140.2 (CH), 48.9 (CH_2), 22.3 (CH_3); GC-MS: *m/z* 342 (M+1).

*(Z)-2-(7-Methyl-2-oxo-2H-pyrido[1,2-a]pyrimidin-3(4H)-ylidene)-N-(p-tolyl)acetamide (**F**):*

2-Oxo-7-methyl-2*H*-pyrido[1,2-*a*]pyrimidin-3 (4*H*)-ylidene acetic acid: 2.18 g; thionyl chloride: 7 ml; *p*-toludine: 2.7 g; ether: 50 ml; yield 3 g (61%); m.p. 252–253°C; IR $(\gamma)_{max}$, cm^{-1}: 3110 (-NH), 1769 (-CO), 1668 (-CO); ^1H NMR (400 MHz, $CDCl_3$, δ, ppm): 4.5 (2H, s, $-CH_2$), 6.8 (1H, d, -CH), aromatic and pyridine ring 7–8 (8H, m, =CH), 9.1 (1H, s(b), -NH), 2.1 (3H, s, $-CH_3$), 2.3 (3H, s, $-CH_3$); ^{13}C NMR (300 MHz, $CDCl_3$, δ, ppm): 169.2 (C=O), 166.0 (amide C=O), ArC (119.4, 120.0, 121.5, 122.4, 129.2, 134.6, 136.8, 142.7, 157.6, 161.6), 141 (CH), 49.6 (CH_2), CH_3 (17.8, 21.3); GC-MS: *m/z* 306 (M+1).

*N-(4-Methoxyphenyl)-2-(2-oxo7-methyl-2H-pyrido[1,2-a]pyrimidin-3(4H)-ylidene)acetamide (**G**):*

2-Oxo-7-methyl-2*H*-pyrido[1, 2-*a*]pyrimidin-3(4*H*)-ylidene acetic acid: 2.18 g; thionyl chloride: 7 ml; *p*-anisidine: 3.1 g; ether: 50 ml; yield 3.2 g (60%); m.p. 248–250°C; IR $(\gamma)_{max}$, cm^{-1}: 3020 (-NH), 1734 (-CO), 1691 (-CO); ^1H NMR (400 MHz, $CDCl_3$, δ, ppm): 4.2 (2H, s, $-CH_2$), 6.5 (1H, d, -CH), 2.1 (3H, s, $-CH_3$), aromatic and pyridine ring 7–8 (8H, m, =CH), 9.2 (1H, s(b), -NH), 3.8 (3H, s, $-OCH_3$); ^{13}C NMR (300 MHz, $CDCl_3$, δ, ppm): 171.2 (C=O), 167.4 (amide C=O), ArC (120.6, 118.5, 142.3, 121.5, 162.4, 157.2, 122.6, 129.9, 114.5, 158.9), 139.4 (CH), 47.3 (CH_2), 19.7, 55.8 (CH_3); GC-MS: *m/z* 322 (M+1).

*N-(4-Chlorophenyl)-2-(2-oxo-7-methyl-2H-pyrido[1,2-a]pyrimidin-3(4H)-ylidene)acetamide (**H**):*

2-Oxo-7-methyl-2*H*-pyrido[1,2-*a*]pyrimidin-3(4*H*)-ylidene acetic acid: 2.18 g; thionyl chloride: 7 ml; *p*-chloroaniline: 3.2 g; ether: 50 ml; yield 3.6 g (67%), m.p. 262– 263°C; IR $(\gamma)_{max}$, cm^{-1}: 3014 (-NH), 1741 (-CO), 1684 (-CO); ^1H NMR (400 MHz, $CDCl_3$, δ, ppm): 4.6 (2H, s, $-CH_2$), 6.8 (1H, d, -CH), aromatic and pyridine ring 7–8 (8H, m, =CH), 9.0 (1H, s(b), -NH), 2.1 (3H, s, $-CH_3$); ^{13}C NMR (300 MHz, $CDCl_3$, δ, ppm): 171.8 (C=O), 165.2 (amide C=O), ArC (104.3, 134.5, 146.01, 159.1, 120.9, 156.2, 135.7, 121.7, 129, 133.3), 139.4 (CH), 53.2 (CH_2) 21.2 (CH_3); GC-MS: *m/z* 327 (M+1).

Molecular docking:

Molecular docking studies are used to predict binding modes of the synthesized compounds with proteins, binding affinity and strength of the protein-ligand complexes. All the newly synthesized compounds were docked individually using Autodock Vina 1.5.6 software. After receiving the modeled three-dimensional structure of bacterial multidrug efflux transporter AcrB (PDB ID: 1T9U) and SpoIIIAH-SpoIIQ complex protein (PDB ID: 3UZ0) to Autodock Vina 1.5.6, it was optimized structurally through adding hydrogen to a protein selected by Kollaman charges. After adding hydrogen the model was saved in PDBQT format. Ligands were prepared for docking studies by adjusting the torsion angles and were saved in PDBQT format. Using PDBSUM, proteins potential binding sites were selected. A grid was generated around the binding site of the protein to identify the XYZ coordinates. Lamarckian Genetic Algorithm (LGA) was selected for docking, freezing, and default parameters used in Autodock Vina 1.5.6. By performing docking studies the binding modes of protein and their binding energies of ligands were estimated. Using SPDBV, the XYZ coordinates of PDB were selected. The interaction of ligand with the 1T9U and 3UZ0 protein

and ligand poses were analyzed and studied based on H-bonding poses to the receptor molecule and van der Waals interaction between the poses and receptor molecule. The unwanted co-factors, chains, and water molecules were removed.

Biological evaluation:

The *in vitro* antibacterial activity screened for the synthesized compounds against *Bacillus subtilis,* and *Escherichia coli* bacterial strains by disc diffusion method against the standard drug Ciprofloxacin (10 μg/disc). Each Petri dish was divided into four quadrants, in 3 quadrants, extract discs such as I (100 mcg), II (200 mcg), III (300 mcg) discs (discs are soaked overnight in extract solution). One quadrant for Standard Ciprofloxacin 5 mcg was placed in each quadrant with the help of sterile forceps. In the refrigerator at 40°C or at room temperature, Petri dishes were set for 1 h for diffusion. Incubate at 370°C for 24 h. The zone of inhibition was observed for different antibiotics. Measured it using a scale or divider or vernier calipers and recorded the average of two diameters of each zone of inhibition.

Results and discussion

The series of *N*-aryl amides of 2-oxo-2*H*-pyrido[1,2-*a*]pyrimidin-3(4*H*)-ylidene acetic acids were prepared usind standard procedure. The amides were prepared in two steps viz.

(i) Conversion of acid to acid chloride using thionylchloride.

(ii) Treatment of acid chloride with various amines to afford *N*-arylamides with moderate yields (Scheme 1).

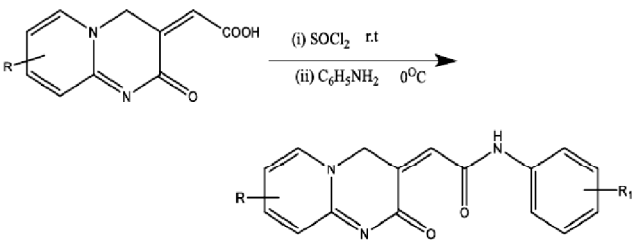

R = H and 5-Me; R_1 = aniline, *p*-toludine, *p*-chloroaniline, *p*-anisidine, naphthylamine

Scheme 1

The synthesized compounds **A-H** were characterized by IR, ^{1}H, and ^{13}C NMR spectral measurements. IR displayed characteristic -NH band at 3243 cm^{-1} and at 1734 cm^{-1}, 1630 cm^{-1} for the two carbonyls. The ^{1}H NMR of the spectrum of the compound **A** exhibited peaks at δ 4.5 and 6.3 corresponding to H4 and H32, respectively. A multiplet at δ 7.0–8.0 was due to the pyridine and benzene nucleus of amine fragment. ^{13}C registered 16 signals, and the mass spectrum displayed M^+ peak at *m/z* 280, confirming the suggested structure.

Antibacterial activity:

By considering Ciprofloxacin (10 μg/disc) as a standard drug, the *in vitro* antibacterial studies of newly synthesized compounds were screened against *Bacillus subtilis* and *Escherichia coli* by disc diffusion method. The study revealed that the tested compounds (**A**-**H**) possess potential antibacterial activity against *Bacillus subtilis* and *Escherichia coli*. The zones of inhibition exhibited by the compounds ranged from 11–13 mm disc (Table 1). The relative susceptibility of

Table 1. Antibacterial activity of synthesised compounds (**A**-**H**) against *Bacillus subtilis* and *Escherichia coli* tested by disc diffusion assay

Compound	Zone of inhibition *Bacillus subtilis*			Standard Ciprofloxacin	Zone of inhibition *Escherichia coli*		
	50 μg/disc	100 μg/disc	150 μg/disc	(10 μg/disc) (mm)	50 μg/disc	100 μg/disc	150 μg/disc
A	11	12	13	25	10	11	12
B	10	11	11		11	12	12
C	12	11	11		13	13	17
D	10	11	11		10	11	12
E	11	12	13		12	11	11
F	11	11	13		11	12	12
G	10	12	12		12	14	12
H	09	10	11		10	11	11

the test microorganisms to a particular antimicrobe were indicated by the diameter of the inhibition zone.

The inhibition results at three concentrations viz. 50 μg, 100 μg, and 150 μg showed that the compounds are sensitive to bacteria at higher concentrations, the sensitivity decreases at lower concentrations. The compound **A** and **E** showed increased sensitivity to the bacteria *Bacillus subtilis,* while *Escherichia coli* compound **C** showed higher activity. The least activity was recorded for compound **B** for both the bacterial strains. The compounds from **A**-**H**, to inhibit bacterial species growth, indicate the compounds' broad-spectrum antibacterial potentials, which makes the synthesized compounds for bioprospecting for antibiotic drugs.

Docking studies:

Molecular docking studies are widely used for the computation of protein-ligand interactions. Docking studies were performed to find the binding affinities and key interactions between the active site of 1T9U and 3UZ0 protein and the newly synthesized compounds, using AutoDock Vina 1.5.6 software. The docking run generated nine different poses for each compound, and the corresponding binding energy scores were generated. The results of all the synthesized compounds and proteins with higher binding energy scores were summarized in Table 2. The compound's stability of the best-docked pose was evaluated by determining the protein's hydrogen-bonding interactions with compounds. Based on

Table 2. Docking results of the designed compounds (**A**-**H**) towards 1T9U and 3UZ0

Compound	PDB	Binding energy Δ*G* (kcal/mol)	PDB	Binding energy Δ*G* (kcal/mol)	Grid X-Y-Z coordinates
A	3UZ0	–10.4	1T9U	–10.7	40, 40, 40
B	3UZ0	–8.8	1T9U	–8.1	40, 40, 40
C	3UZ0	–9.3	1T9U	–9.2	40, 40, 40
D	3UZ0	–9	1T9U	–8.4	40, 40, 40
E	3UZ0	–8.9	1T9U	–8.6	40, 40, 40
F	3UZ0	–9	1T9U	–8.7	40, 40, 40
G	3UZ0	–9	1T9U	–8.5	40, 40, 40
H	3UZ0	–9.3	1T9U	–9.1	40, 40, 40

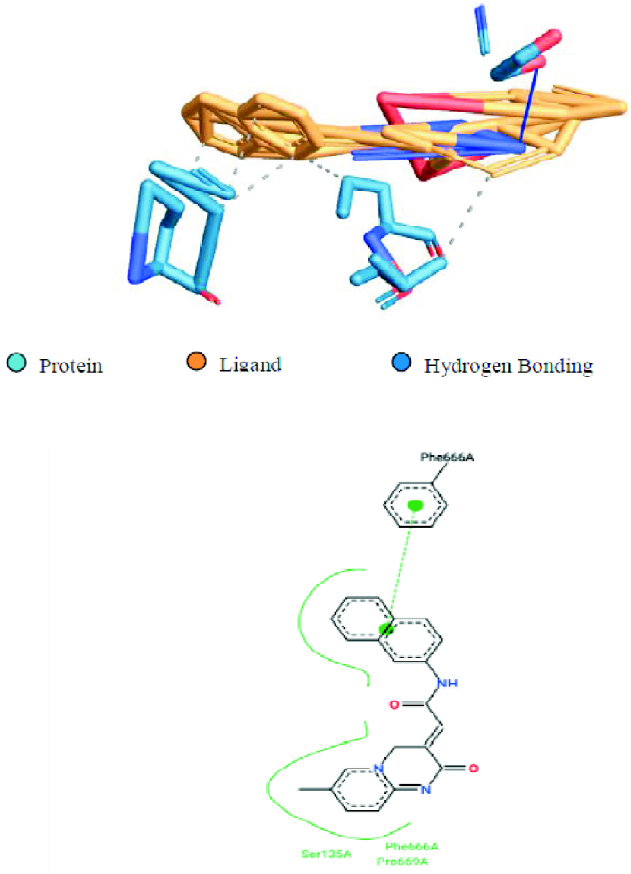

Fig. 1. 2D and 3D structure of (*Z*)-*N*-(naphthalene-2-yl)-2-(2-oxo-7-methyl-2*H*-pyrido[1,2-*a*]pyrimidin-3(4*H*)-ylidene)acetamide docked with protein 1T9U.

these factors, among all the compounds (*Z*)-*N*-(naphthalene-2-yl)-2-(2-oxo-7-methyl-2*H*-pyrido[1,2-*a*]pyrimidin-3(4*H*)-ylidene)acetamide shows the highest binding energy with 1T9U and 3UZ0 protein with binding energy Δ*G* –10.7 and –10.4 (kcal/mol) (Figs. 1 and 2). The docking score and H-bond interaction, van der Waal forces, were done for all the synthesized compounds. Binding energies were calculated; it consists of van der Waal forces, H-bonding, π-π interactions, cation-π interactions, etc. The hydrogen bonding distance for (*Z*)-*N*-(naphthalene-2-yl)-2-(2-oxo-7-methyl-2*H*-pyrido[1,2-*a*]pyrimidin-3(4*H*)-ylidene)acetamide with the proteins are 3 and 3.21 Å and donor angles are 134.72° and 114.91° respectively.

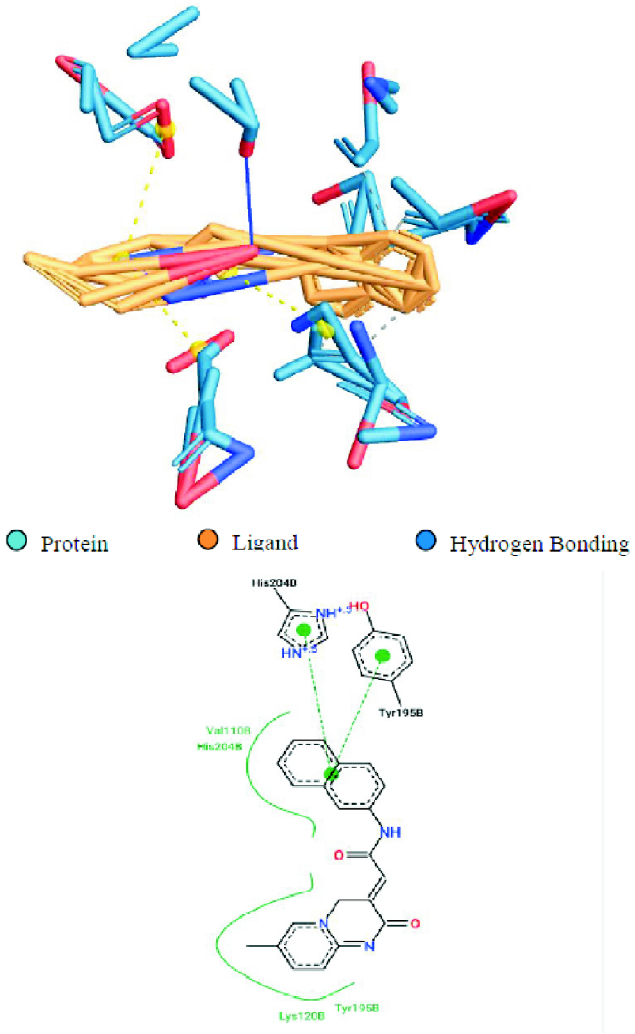

Fig. 2. 2D and 3D structure of (*Z*)-*N*-(naphthalene-2-yl)-2-(2-oxo-7-methyl-2*H*-pyrido[1,2-*a*]pyrimidin-3(4*H*)-ylidene)acetamide docked with protein 3UZ0.

Conclusion

In summary, a series of novel *N*-aryl amides of pyrido[1, 2-*a*]pyrimidin-2-ones were prepared and evaluated for their antibacterial activity against *Bacillus subtilis* and *Escherichia coli*, and Molecular docking studies also performed in which 3UZ0 and 1T9U as the target protein. Based on the result, we claim that (*Z*)-*N*-(naphthalene-2-yl)-2-(2-oxo-7-methyl-2*H*-pyrido[1,2-*a*]pyrimidin-3(4*H*)-ylidene)acetamide could serve as an effective antimicrobial compound to treat bacterial infections. We believe that this work on this unique moiety to explore its activities further helps humankind synthesize new drugs.

References

1. S. D. Vachala, *Der Pharma Chemica,* 2012, **4(1)**, 255.
2. Toshiaki Sasada, Fuminori Kobayashi, Norio Sakai and Takeo Konakahara, *Org. Lett.,* 2009, **11**, 2161.
3. Ch. Pratyusha, G. Poornima, K. Sandhya Rani, A. Krishnaveni, B. Brahmaiah, Sreekanth Nama, *International Journal of Pharmacy Review & Research,* 2013, **3(2)**, 86.
4. Vivek Jagadeesan Sharavanan, Muthusaravanan Sivaramakrishnan, Ram Kothandan, Shanmugaprakash Muthusamy and Kumaravel Kandaswamy, *Pharmacognosy Journal*, 2019, **11(2)**, 278.
5. Isabella A. Guedes and Camila S. de Magalhães and Laurent E. Dardenne, *Advances in Biophysics in Latin America*, 2014, **6**, 75.
6. Oleg Trott and Arthur J. Olson, *Journal of Computational Chemistry,* 2010, **31**, 455.
7. Stefano Forli, Ruth Huey, Michael E. Pique, Michel F. Sanner, David S. Goodsell and Arthur J. Olson, *Nature Protocols*, 2016, **11(5)**, 905.
8. Sharulatha Venugopal and Sivakamasundari Sundaram, *J. Heterocyclic Chem.*, 2016, **53**, 882.
9. Srinivasa Rao Dasari, Subbaiah Tondepu, Lakshmana Rao Vadali and Naresh Varma Seelam, *Asian J. Chem.*, 2019, **31(12)**, 2733.
10. Panneerselvam Kalaivani, Jayaraman Arikrishnan and Mannuthusamy Gopalakrishnan, *Asian J. Chem.*, 2020, **32(6)**, 1437.
11. Lucia Veltri, Salvatore V. Giofre, Perry Devo, Roberto Romeo, Adrian P. Dobbs and Bartolo Gabriele, *J. Org. Chem.,* 2018, **83(3)**, 1680.

Avinashilingam Institute for Home Science and Higher Education for Women
(Deemed to be University Estd. u/s 3 of UGC Act 1956, Category A by MHRD)
Re-accredited with 'A++' Grade by NAAC.CGPA 3.65/4, Category I by UGC
Coimbatore – 641 043, Tamil Nadu, India

PLAGIARISM CHECK REPORT (THESES)

1.	Name of the Research Scholar	A. Abinaya
2.	Roll No. and Year of Registration	17PHCHF001, 2017
3.	Department	Chemistry
4.	Name of the Research Guide	Dr. V. Sharulatha
5.	Title of the Thesis / Dissertation	Inverse Electron Demand Diels Alder reaction of Pyrido [1,2-a]pyrimidine-2-ones-Experimental and Theoretical Investigation and Antibacterial activity of synthesized Adducts
6.	Similarity Content (%) Identified	**9%**
7.	Software Used	Turnitin
8.	Date of Verification	31-03-2023

Note : The report is excluding 14 Consecutive words, Review of Literature and Quoted Materials.

Checked by :

K. Jakgi 31/3/2023
for **Information Scientist**

A. Abinaya
Research Scholar

31.3.23
Assistant Librarian

Research Guide

Date: 31-03-2023

Digital Receipt

This receipt acknowledges that Turnitin received your paper. Below you will find the receipt information regarding your submission.

The first page of your submissions is displayed below.

Submission author:	Abinaya A
Assignment title:	New 2022
Submission title:	Inverse Electron Demand Diels Alder reaction of Pyrido [1,2-...
File name:	Plagarism-30.03.2023_1.docx
File size:	13.48M
Page count:	138
Word count:	13,587
Character count:	76,501
Submission date:	31-Mar-2023 05:31PM (UTC+0530)
Submission ID:	2051976183

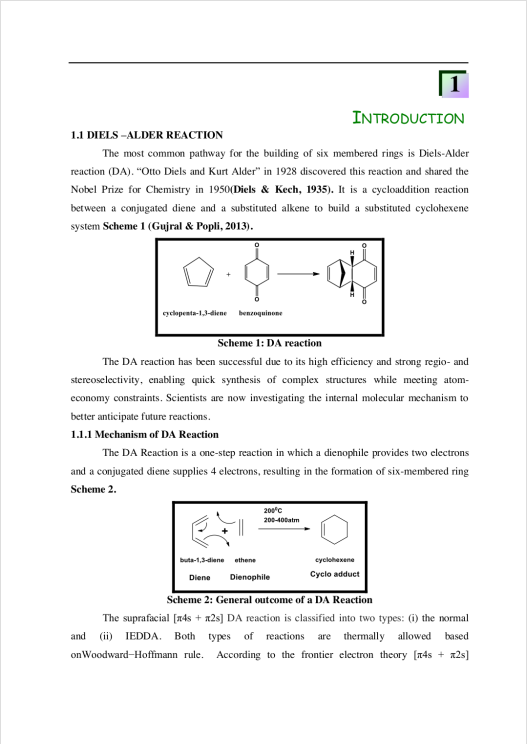

1

INTRODUCTION

1.1 DIELS –ALDER REACTION

The most common pathway for the building of six membered rings is Diels-Alder reaction (DA). "Otto Diels and Kurt Alder" in 1928 discovered this reaction and shared the Nobel Prize for Chemistry in 1950(**Diels & Kech, 1935).** It is a cycloaddition reaction between a conjugated diene and a substituted alkene to build a substituted cyclohexene system **Scheme 1 (Gujral & Popli, 2013).**

cyclopenta-1,3-diene benzoquinone

Scheme 1: DA reaction

The DA reaction has been successful due to its high efficiency and strong regio- and stereoselectivity, enabling quick synthesis of complex structures while meeting atom-economy constraints. Scientists are now investigating the internal molecular mechanism to better anticipate future reactions.

1.1.1 Mechanism of DA Reaction

The DA Reaction is a one-step reaction in which a dienophile provides two electrons and a conjugated diene supplies 4 electrons, resulting in the formation of six-membered ring **Scheme 2.**

200°C
200-400atm
buta-1,3-diene ethene cyclohexene
Diene Dienophile Cyclo adduct

Scheme 2: General outcome of a DA Reaction

The suprafacial [π4s + π2s] DA reaction is classified into two types: (i) the normal and (ii) IEDDA. Both types of reactions are thermally allowed based onWoodward–Hoffmann rule. According to the frontier electron theory [π4s + π2s]

Inverse Electron Demand Diels Alder reaction of Pyrido [1,2-a] Pyrimidine-2-ones- Experimental and Theoretical Investigation and anti-Bacterial Activity of Synthesized Adducts

by Abinaya A

Submission date: 31-Mar-2023 05:31PM (UTC+0530)
Submission ID: 2051976183
File name: Plagarism-30.03.2023_1.docx (13.48M)
Word count: 13587
Character count: 76501

Inverse Electron Demand Diels Alder reaction of Pyrido [1,2-a] Pyrimidine-2-ones-Experimental and Theoretical Investigation and anti-Bacterial Activity of Synthesized Adducts

ORIGINALITY REPORT

9%	6%	7%	1%
SIMILARITY INDEX	INTERNET SOURCES	PUBLICATIONS	STUDENT PAPERS

PRIMARY SOURCES

1	acikbilim.yok.gov.tr Internet Source	1%
2	dspace.uzhnu.edu.ua Internet Source	1%
3	Venugopal, Sharulatha, and Sivakamasundari Sundaram. "Simple and Efficient Synthesis of 2-Oxo-2H-Pyrido[1,2-a]Pyrimidin-3(4H)-Ylidene Acetic Acid and Its Rearrangement in Presence of Acid Media : Synthesis of Pyrido1,2-Apyrimidines", Journal of Heterocyclic Chemistry, 2015. Publication	1%
4	www.mdpi.com Internet Source	1%
5	Li, Z.. "Novel thiazonaphthalimides as efficient antitumor and DNA photocleaving agents: Effects of intercalation, side chains, and substituent groups", Bioorganic & Medicinal Chemistry, 20050815	<1%